American Mineralogist, Volume 60, pages 423–434, 1975

The Effect of Ca-Fe Substitution on the Clinopyroxene Crystal Structure

YOSHIKAZU OHASHI,

Geophysical Laboratory, Carnegie Institution of Washington, Washington, D. C. 20008

CHARLES W. BURNHAM,

Department of Geological Sciences, Harvard University, Cambridge, Massachusetts 02138

AND LARRY W. FINGER

Geophysical Laboratory, Carnegie Institution of Washington, Washington, D. C. 20008

Abstract

The major structural change resulting from Ca-Fe substitution in four clinopyroxenes of intermediate composition between hedenbergite and ferrosilite, measured at room temperature, is in the size and shape of the *M*2 polyhedron, whereas the *M*1 polyhedron remains essentially unchanged. The decrease in the average size of the *M*2 polyhedron associated with a compositional change from hedenbergite to ferrosilite causes kinking of the tetrahedral chain and concomitant increases in the out-of-plane tilting of the basal face of the tetrahedron. As the *M*2 polyhedron decreases further in size, the space group changes from $C2/c$ to $P2_1/c$ at about $Fs_{80}Wo_{20}$ composition. When the composition changes from $Fs_{88}Wo_{12}$ to $Fs_{100}Wo_0$, the *A* chain extends and finally reverses its kink direction. The anisotropic temperature factors for these intermediate compositions may be explained as a result of the effects of positional disorder.

Introduction

Most minerals can form solid solutions, either limited or complete, and thus some sites in the unit cells of minerals are occupied statistically by more than one atomic species. If there is a large difference in the ionic radii of the atoms occupying the site, the crystal structure may change with a change in occupancy of the site and thus in the apparent size of the coordination polyhedron. One of the best mineralogical examples of multiple occupancy is augite-pigeonite, where substitution of Ca for Fe or Mg is involved.

In the pyroxene quadrilateral (diopside-enstatite-ferrosilite-hedenbergite system) the clinopyroxene space groups are $P2_1/c$ for Ca-poor (pigeonite) compositions and $C2/c$ for Ca-rich (augite) compositions at room temperature. The major differences between the $P2_1/c$ and $C2/c$ structures are that (1) there is only one crystallographically distinct silicate chain in the $C2/c$ structure, whereas two types of the chains exist in the $P2_1/c$ structure, and (2) the *M*2 site[1] is eight-coordinated in the $C2/c$ end members (diopside: Clark, Appleman, and Papike, 1969; hedenbergite: Veblen, 1969, and Cameron *et al*, 1973) and six-coordinated in the $P2_1/c$ end members (clinoferrosilite: Burnham, 1967; clinoenstatite: Morimoto, Appleman, and Evans, 1960).

In clinopyroxenes of intermediate composition, the *M*2 site is very irregular as a result of multiple occupancy of the large Ca and small Fe or Mg atoms in the site. In a structural refinement of a pigeonite, $Mg_{0.39}Fe_{0.52}Ca_{0.09}SiO_3$ from Mull, Scotland, Morimoto and Güven (1970) reported a very irregular *M*2 coordination polyhedron, which they concluded was an average of eight and six coordinations. Güven (1969) studied the relationship between the average size of *M*2 and kinking of the

[1] Nomenclature for the pyroxenes is that proposed by Burnham *et al* (1967).

tetrahedral chain. Takeda (1972) discussed variation of $M2$–O bonds in clinopyroxenes as a function of Ca content and showed that the $M2$ polyhedron becomes very irregular, thus highly unstable, in the middle of the solid solution. He proposed that irregularity of the $M2$ polyhedral shape provided a structural explanation for the presence of a miscibility gap. In their crystal structural study of six end-member clinopyroxenes at high temperatures, Cameron *et al* (1973) explained the increased solid solution between the Ca-poor and Ca-rich clinopyroxenes at high temperature by the change in $M2$ coordination associated with the $P2_1/c$–$C2/c$ phase transition.

The present study is concerned primarily with the effects of chemical substitution on the structure studied at room temperature. To eliminate the structural effects of possible changes of Mg-Fe distribution in the cation sites, the binary join hedenbergite ($CaFeSi_2O_6$)–clinoferrosilite ($Fe_2Si_2O_6$) was selected. Therefore, these structures reflect solely a difference between Ca and Fe contents. Furthermore, if the $M1$ site on the join studied is occupied only by Fe atoms, as expected from its polyhedral size, it is possible to isolate the effects of changes of the $M2$ site on the other parts of the structure, especially the tetrahedral chain configuration.

Experimental

Unit Cell and Space Group

Synthetic single crystals of clinopyroxenes on the hedenbergite–clinoferrosilite join were kindly supplied by Dr. D. H. Lindsley. Synthesis techniques were described by Lindsley and Munoz (1969, Appendix). Crystals of $Fs_{85}Wo_{15}$,[2] $Fs_{80}Wo_{20}$, $Fs_{75}Wo_{25}$ (all synthesized at 20 kbar and 950°C), and $Fs_{65}Wo_{35}$ (6 kbar and 1140°C) have been examined using the Buerger precession camera. Class b reflections ($h + k$ = odd) are exhibited by $Fs_{85}Wo_{15}$ and some crystals of $Fs_{80}Wo_{20}$, whereas long-exposure photographs of $Fs_{65}Wo_{35}$, $Fs_{70}Wo_{30}$, and the other crystals of $Fs_{80}Wo_{20}$ do not show these b reflections. Thus the (metastable) boundary at room temperature between the space groups $P2_1/c$ and $C2/c$ is close to the $Fs_{80}Wo_{20}$ composition on the join hedenbergite–ferrosilite. At low pressures the clinopyroxene of this composition is not stable relative to the assemblage fayalite + tridymite (Bowen, Schairer, and Posnjak, 1933; Lindsley and Munoz, 1969). No exsolved phases are detected on long-exposure precession photographs, and thus the crystals are considered to be homogeneous.

TABLE 1. Unit-Cell Parameters and Unit-Cell Volume of Ca-Fe Clinopyroxenes

	$Fs_{65}Wo_{35}$	$Fs_{75}Wo_{25}$	$Fs_{80}Wo_{20}$	$Fs_{85}Wo_{15}$
a (Å)	9.812(1)*	9.781(2)	9.760(6)	9.779(1)
b (Å)	9.049(1)	9.072(2)	9.057(8)	9.085(1)
c (Å)	5.233(1)	5.246(2)	5.234(3)	5.258(1)
β (deg.)	105.34(1)	106.35(2)	106.28(5)	107.39(1)
V (Å^3)	448.1(1)	446.2(3)	444.1(6)	445.9(2)
Method**	BW	BW	FD	BW

*Parenthesized figures represent the estimated standard deviation (esd) in terms of least units cited for the value to their immediate left, thus for 9.812(1) read 9.812 ± 0.001.
**BW: back-reflection Weissenberg camera.
FD: four-circle diffractometer.

[2] Compositions are in molecular proportions of Fs ($FeSiO_3$) and Wo ($CaSiO_3$). Crystals of $Fs_{65}Wo_{35}$ and $Fs_{75}Wo_{25}$ were examined using the electron microprobe. No inhomogeneities were observed with the error in composition estimated to be less than 3 mole percent Fs.

Unit-cell parameters of crystals other than $Fs_{80}Wo_{20}$ were measured using a back-reflection precision Weissenberg camera. Data for both $CuK\alpha_1$ and $K\alpha_2$ wavelengths were refined by the least-squares method and included corrections for film shrinkage, camera eccentricity, and specimen absorption (Burnham, 1962). Unit-cell parameters for $Fs_{80}Wo_{20}$ were determined by a lattice-constant refinement subroutine for a four-circle diffractometer. This subroutine, which is a part of the Geophysical Laboratory diffractometer system, has some new features: auto-centering of reflections and least-squares refinement of the orientation matrix from which the unit-cell parameters (Table 1) are calculated (Finger, unpublished; Gabe, Alexander, and Goodman, 1970). Analysis of the clinopyroxene lattice deformation due to chemical substitution on this join is given elsewhere (Ohashi and Burnham, 1973).

Measurement and Reduction of X-Ray Intensity Data

Intensity data were collected using a computer-controlled Picker four-circle diffractometer with Nb-filtered Mo$K\alpha$ radiation. Reflections in one quadrant of reciprocal space within the range 0.1 to 0.8 of $\sin\theta/\lambda$ were measured employing ω-2θ scans. The observed intensities were corrected for Lorentz and polarization effects and for absorption using the numerical integration techniques of Burnham (1966). In addition, the secondary extinction factor of Zachariasen (1968) was calculated for the $Fs_{75}Wo_{25}$ and $Fs_{80}Wo_{20}$ crystals.

The crystal of $Fs_{85}Wo_{15}$ is twinned on (100). Therefore, the $hk0$ reflections contain superimposed contributions from both twin components. By com-

TABLE 2. Crystal and Refinement Data for Ca-Fe Clinopyroxenes

	$Fs_{65}Wo_{35}$	$Fs_{75}Wo_{25}$	$Fs_{80}Wo_{20}$	$Fs_{85}Wo_{15}$
Space group	$C2/c$	$C2/c$	$C2/c$	$P2_1/c$
Size of crystal (mm)	0.13×0.20 ×0.39	0.03×0.04 ×0.21	0.09×0.11 ×0.14	0.07×0.08 ×0.29
Linear absorption coefficient (cm^{-1}) for MoKα	56.28	60.74	63.14	64.98
Range of transmission factor (%)	31-56	78-85	57-67	60-70
Number of reflections used in refinement	967	492	795	1144
Residual factor (%)*				
R	4.3	5.8	4.9	6.2
R(wtd.)	3.7	5.5	5.3	4.2

*$R = \Sigma||F_o| - |F_c||/\Sigma|F_o|$.

$R(\text{wtd.}) = [\Sigma w(|F_o| - |F_c|)^2/\Sigma w|F_o|^2]^{1/2}$.

paring the intensities of the two twin components for several *hkl* reflections that were resolved, the volume of one component was estimated as 95.4 percent of the crystal volume, and the proper correction was made for the unresolved *hk*0 reflections.

TABLE 3. Atomic Positional Parameters and Equivalent Isotropic Temperature Factors for Ca-Fe Clinopyroxenes*

		$Fs_{65}Wo_{35}$ ($C2/c$)	$Fs_{75}Wo_{25}$ ($C2/c$)	$Fs_{80}Wo_{20}$ ($C2/c$)	$Fs_{85}Wo_{15}$ ($P2_1/c$)	
					A chain	B chain
M1 (Fe)	x	0	0	0	0.2512(2)	
	y	0.9064(1)†	0.9047(3)	0.9050(1)	0.6563(1)	
	z	1/4	1/4	1/4	0.2634(4)	
	$B_{eq.}$**	0.44(3)	0.80(4)	0.64(2)	0.67(1)	
M2	Ca occ.††	0.7	0.5	0.4	0.3	
	Fe occ.	0.3	0.5	0.6	0.7	
	x	0	0	0	0.2534(3)	
	y	0.2908(1)	0.2747(3)	0.2751(1)	0.0182(1)	
	z	1/4	1/4	1/4	0.2443(5)	
	$B_{eq.}$	1.31(2)	1.85(6)	1.78(3)	1.46(2)	
Si	x	0.2901(1)	0.2936(2)	0.2937(1)	0.0461(3)	0.5455(3)
	y	0.0910(1)	0.0898(3)	0.0891(1)	0.3387(4)	0.8373(4)
	z	0.2370(1)	0.2434(4)	0.2440(2)	0.2569(5)	0.2436(5)
	$B_{eq.}$	0.41(1)	0.75(4)	0.65(2)	0.73(4)	0.63(4)
O1	x	0.1207(2)	0.1207(6)	0.1216(3)	0.0729(6)	0.3719(7)
	y	0.0895(3)	0.0893(8)	0.0893(3)	0.3407(10)	0.8360(12)
	z	0.1526(4)	0.1517(11)	0.1535(6)	0.1601(12)	0.1499(14)
	$B_{eq.}$	0.63(3)	0.82(8)	0.78(4)	0.60(9)	0.95(11)
O2	x	0.3658(3)	0.3706(7)	0.3712(4)	0.1182(9)	0.6280(7)
	y	0.2448(3)	0.2426(7)	0.2417(3)	0.6948(11)	0.9873(9)
	z	0.3317(5)	0.3496(16)	0.3480(8)	0.3423(17)	0.3656(16)
	$B_{eq.}$	1.10(4)	1.75(14)	1.53(6)	1.71(14)	0.99(12)
O3	x	0.3505(2)	0.3520(7)	0.3517(3)	0.1002(7)	0.6038(8)
	y	0.0222(2)	0.0255(7)	0.0261(4)	0.2299(10)	0.7192(9)
	z	-0.0055(4)	-0.0043(14)	-0.0020(6)	0.5172(14)	0.4983(13)
	$B_{eq.}$	0.70(3)	1.26(10)	1.14(5)	1.95(15)	1.13(12)

*Fractional coordinates refer to the conventional origin in those space groups. Coordinate translations between two origins are $x_p = x_c \pm 1/4$, $y_p = y_c \pm 1/4$, and $z_p = z_c$.

**$B_{eq.}$ = Equivalent isotropic temperature factor computed from anisotropic temperature factors, β_{ij}, according to $B_{eq.} = \frac{4}{3}\sum_i\sum_j \beta_{ij}\, a_i \cdot a_j$ (Hamilton, 1959).

†Parenthesized figures represent the estimated standard deviation (esd) in terms of least units cited for the value to their immediate left, thus for 0.9064(1) read 0.9064 ± 0.0001.

††Occupancy of the M2 site is fixed by bulk chemical composition (see text).

Refinement Procedures

Throughout all refinements, the least-squares program REFINE of Finger was used on the IBM 370 and the UNIVAC 1108 computers. Atomic scattering factors were those of Fe^{2+}, Ca^{2+}, Si^{4+}, and O^- given by Cromer and Mann (1968) with the anomalous dispersion coefficients of Cromer (1965).

Least-squares refinements of $Fs_{85}Wo_{35}$ and $Fs_{85}Wo_{15}$ were initiated with atomic parameters of hedenbergite (Veblen, 1969) and clinoferrosilite (Burnham, 1967), respectively. Refined parameters of $Fs_{65}Wo_{35}$ and $Fs_{75}Wo_{25}$, respectively, were used as initial parameters of $Fs_{75}Wo_{25}$ and $Fs_{80}Wo_{20}$. Reflections were weighted according to $w = 1/\sigma^2$, where σ is the estimated standard deviation of the observed structure factor. Reflections were rejected from least-squares refinement if the intensity was below two standard deviations of the observed intensity based on counting statistics. At the later stage of least-squares refinement, reflections with $\Delta F = F_o - F_c$ greater than 6 were also rejected.

In each structure the atomic positions, anisotropic temperature factor coefficient, and a scale factor were refined. In addition, the isotropic extinction parameter of Zachariasen (1968) was refined for the $Fs_{75}Wo_{25}$ and $Fs_{80}Wo_{20}$ data sets. The correction for the twinning in $Fs_{85}Wo_{15}$ was tested by refining a separate scale factor for (*hk*0). The resulting values were essentially identical, confirming the validity of the prior correction. No strong correlations between parameters were found for the $C2/c$ structural refinements. However, the A and B chains in the $P2_1/c$ structure are in general highly correlated: -0.75 between β_{12}'s of SiA and SiB and -0.71 between y's of O1A and O1B were found to be the strongest correlations.

From an ionic size consideration, all Ca atoms are assumed to occupy the larger $M2$ site. Thus, for example, the occupancy of cation sites for $Fs_{85}Wo_{15}$ is 100 percent Fe^{2+} in the $M1$ site and (70 percent Fe^{2+} + 30 percent Ca) in the $M2$ site.

Data for the crystals and refinements are summarized in Table 2. The final positional parameters and temperature factors are given in Tables 3 and 4, respectively. Tables of observed and calculated structure factors may be ordered.[3]

[3] To receive a copy of these structure factor tables, order document AM-75-001 from the Business Office, Mineralogical Society of America, suite 1000 lower level, 1909 K Street, N.W., Washington, D. C. 20006. Please remit $1.00 for the microfiche.

TABLE 4. Anisotropic Temperature Factors for Ca-Fe Clinopyroxenes*

		$Fs_{65}Wo_{35}$	$Fs_{75}Wo_{25}$	$Fs_{80}Wo_{20}$	$Fs_{85}Wo_{15}$	
M1	β_{11}	0.0017(1)**	0.0019(2)	0.0017(1)	0.0018(1)	
	β_{22}	0.0010(1)	0.0025(2)	0.0015(1)	0.0022(1)	
	β_{33}	0.0038(2)	0.0093(8)	0.0093(3)	0.0067(3)	
	β_{12}	0	0	0	0.0002(2)	
	β_{13}	0.0008(1)	0.0012(3)	0.0022(1)	0.0012(1)	
	β_{23}	0	0	0	0.0002(4)	
M2	β_{11}	0.0025(1)	0.0026(3)	0.0022(1)	0.0020(1)	
	β_{22}	0.0074(1)	0.0100(4)	0.0105(2)	0.0082(1)	
	β_{33}	0.0050(3)	0.0105(11)	0.0105(4)	0.0079(3)	
	β_{12}	0	0	0	-0.0001(2)	
	β_{13}	0.0001(1)	-0.0007(4)	0.0010(2)	-0.0001(1)	
	β_{23}	0	0	0	0.0007(4)	
				A chain	B chain	
Si	β_{11}	0.0014(1)	0.0018(2)	0.0015(1)	0.0012(2)	0.0021(2)
	β_{22}	0.0012(1)	0.0019(2)	0.0016(1)	0.0028(3)	0.0014(3)
	β_{33}	0.0038(2)	0.0103(9)	0.0106(4)	0.0083(7)	0.0078(7)
	β_{12}	-0.0002(1)	-0.0001(3)	-0.0003(1)	0.0003(3)	-0.0007(3)
	β_{13}	0.0011(1)	0.0019(3)	0.0028(1)	0.0009(3)	0.0020(4)
	β_{23}	-0.0005(1)	-0.0000(6)	-0.0008(2)	-0.0008(5)	-0.0007(5)
O1	β_{11}	0.0021(2)	0.0020(5)	0.0016(2)	0.0013(5)	0.0023(2)
	β_{22}	0.0016(2)	0.0023(5)	0.0024(3)	0.0021(7)	0.0035(8)
	β_{33}	0.0056(7)	0.0113(23)	0.0106(10)	0.0048(18)	0.0103(23)
	β_{12}	0.0003(2)	0.0001(7)	0.0002(3)	-0.0000(7)	0.0000(8)
	β_{13}	0.0011(3)	0.0024(9)	0.0019(4)	-0.0008(8)	0.0026(11)
	β_{23}	0.0002(5)	-0.0025(15)	0.0000(5)	0.0002(13)	-0.0010(16)
O2	β_{11}	0.0039(2)	0.0036(7)	0.0043(3)	0.0055(8)	0.0017(6)*
	β_{22}	0.0023(2)	0.0025(7)	0.0025(3)	0.0041(9)	0.0017(8)
	β_{33}	0.0134(9)	0.0355(62)	0.0287(16)	0.0232(33)	0.0192(28)
	β_{12}	-0.0013(2)	-0.0006(6)	-0.0018(3)	0.0001(8)	-0.0019(6)
	β_{13}	0.0039(4)	0.0070(14)	0.0088(6)	0.0076(14)	0.0027(11)
	β_{23}	-0.0022(4)	-0.0012(15)	-0.0040(6)	-0.0005(15)	-0.0035(13)
O3	β_{11}	0.0018(2)	0.0021(5)	0.0018(3)	0.0006(6)	0.0026(8)
	β_{22}	0.0030(2)	0.0058(7)	0.0053(4)	0.0166(12)	0.0056(9)
	β_{33}	0.0069(7)	0.0111(22)	0.0120(11)	0.0193(25)	0.0098(32)
	β_{12}	-0.0000(2)	0.0007(6)	-0.0001(3)	0.0012(6)	-0.0007(6)
	β_{13}	0.0008(3)	0.0013(9)	0.0029(4)	0.0001(11)	0.0021(11)
	β_{23}	-0.0016(4)	-0.0029(13)	-0.0032(5)	0.0105(14)	0.0015(11)

*Anisotropic temperature factors, β_{ij}, are in the form of

$$\exp - (\beta_{11}h^2 + \beta_{22}k^2 + \beta_{33}\ell^2 + 2\beta_{12}hk + 2\beta_{13}h\ell + 2\beta_{23}k\ell)$$

**Parenthesized figures represent the estimated standard deviation (esd) in terms of least units cited for the value to their immediate left, thus for 0.0017(1) read 0.0017 ± 0.0001.

Results and Discussion

M1 and M2 Sites

Interatomic distances for the *M*1 and *M*2 sites are given in Table 5. The *M*1–O bond distances (Fig. 1) and the polyhedral volume (Table 5) both show essentially no change for the *M*1 site with Ca-Fe substitution. This observation seems to verify the assumption that all calcium is restricted to *M*2 on the join studied. As characterized by the quadratic elongation and the angle variance given in Table 5 (quantities proposed by Robinson, Gibbs, and Ribbe, 1971, as measures of polyhedral distortion), the *M*1 polyhedron deviates slightly more from an ideal octahedron on the Fe-rich side. It is, however, still much more regular than the *M*2 polyhedron (quadratic elongation = 1.06 and angle variance = 164° for *M*2 in clinoferrosilite).

The *M*2 site changes from eight-coordinated in hedenbergite to six-coordinated in ferrosilite. Details of this change are one of the main points of interest in the present study. With increasing Fe content, the *M*2 polyhedral volume decreases and the *M*2–O1 and *M*2–O2 distances also decrease (Fig. 1), as a result of substitution of smaller Fe atoms for larger Ca atoms. On the other hand, all four *M*2–O3 distances increase when the composition changes from $Fs_{50}Wo_{50}$ to $Fs_{80}Wo_{20}$. In the $P2_1/c$ region these bonds split into two groups, one increasing and the other decreasing with further Fe enrichment. In clinoferrosilite only six *M*2–O distances are less than 3 Å, the approximate value of the shortest oxygen-oxygen or metal-metal distance.

This change of the *M*2 coordination can be visualized with the aid of Figure 2. The changes of the *M*2–O distances occur as a consequence of a rotation of the O3*A*1–O3*A*2 and O3*B*1–O3*B*2 vectors in

TABLE 5. Interatomic Distances *M*1–O and *M*2–O in Ca-Fe Clinopyroxenes

		$Fe_{65}Wo_{35}$	$Fe_{75}Wo_{25}$	$Fe_{80}Wo_{20}$	$Fe_{85}Wo_{15}$
	M1 Site				
1	M1–O1A1	2.127(2)*	2.103(6)	2.113(3)	2.116(7)
2	–O1B2				2.103(8)
3	–O1A2	2.175(2)	2.192(7)	2.187(3)	2.225(8)
4	–O1B1				2.174(9)
5	–O2A	2.086(2)	2.101(7)	2.096(3)	2.109(9)
6	–O2B				2.110(8)
Mean		2.129	2.132	2.132	2.140
Quad. Elong.**		1.0062	1.0057	1.0053	1.0065
Ang. Var. (deg.^{2})**		13.5	17.7	16.9	20.6
Polyhedral Volume (Å^3)		12.8	12.8	12.8	12.9
	M2 Site				
1	M2–O1A	2.302(2)	2.198(6)	2.197(3)	2.179(8)
2	–O1B				2.162(9)
3	–O2A	2.259(3)	2.127(8)	2.133(4)	2.135(10)
4	–O2B				2.033(9)
5	–O3A1	2.765(2)	2.844(8)	2.842(4)	2.800(9)
6	–O3B2				2.889(8)
7	–O3A2	2.700(2)	2.822(7)	2.817(4)	3.048(8)
8	–O3B1				2.825(7)
Mean of 4, Nbr†		2.281	2.163	2.165	2.127
Mean of 4, Br†		2.733	2.833	2.830	2.891
Mean of 8		2.507	2.498	2.497	2.509
Polyhedral Volume (Å^3)		25.7	24.7	24.7	24.8 [8-coord.] 18.1 [7-coord.]

*Parenthesized figures represent the estimated standard deviation (esd) in terms of least units cited for the value to their immediate left, thus for 2.127(2) read 2.127 ± 0.002.

**Octahedral quadratic elongation (Robinson et al., 1971) defined by $\sum_{i=1}^{6} (\ell_i/\ell_o)^2/6$, where ℓ_o is the center-to-vertex distance for an ideal octahedron whose volume is equal to that of the observed M1 octahedron.

Octahedral angle variance defined by $\sum_{i=1}^{12} (\theta_i - 90)^2/11$.

†Nbr: nonbridging oxygen atoms (O1 and O2) and Br: bridging oxygen atom (O3).

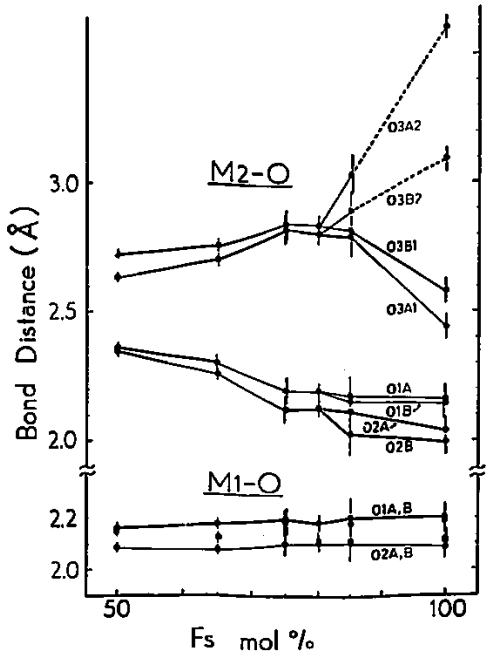

FIG. 1. Variation of $M1$–O and $M2$–O interatomic distances with ferrosilite content in Ca-Fe clinopyroxenes. Error bars represent ±1 standard deviation. Data for hedenbergite and clinoferrosilite are after Cameron *et al* (1973) and Burnham (1967), respectively. See Figure 2 for details of $M2$ coordination geometry.

(100) accompanied by relative movements of the O1 and O2 atoms toward $M2$. Rotations of the O3$B1$–O3$B2$ vector, for example, result in an increase of $M2$–O3$B2$ and decrease of $M2$–O3$B1$.

The question arises whether the structural changes described above are real changes of polyhedral geometry. If the shape of any given $M2$ coordination polyhedron is governed only by the species of atom (Ca or Fe) occupying that site (case 1), there will be only two possible types of $M2$ polyhedra in the pyroxenes studied, one found in hedenbergite and the other in clinoferrosilite, and the crystal structure of an intermediate phase obtained by X-ray diffraction would be an average of the two. In case 1, therefore, discussion of the $M2$ polyhedral geometry for intermediate compositions would have little physical meaning because the average would not represent the real structure. On the other hand, if the shape of any given $M2$ polyhedron is determined not only by the atomic species in the site but also by those in the neighboring $M2$ sites (case 2), then there are various possibilities for the $M2$ polyhedral shapes. In this case structural refinement of the X-ray data would still yield an average structure, but it would approximate the true structure more closely than in case 1.

Results of a Mössbauer study on these clinopyroxenes (Dowty and Lindsley, 1973) may help to resolve these two cases. The quadrupole splitting can be correlated with the degree of polyhedral distortion and thus it reflects primarily a short-range atomic arrangement around the *iron* atom. The change of the $M2$ quadrupole splitting (Fig. 3) indicates that the local configuration around the ferrous ion changes as the bulk chemical composition changes. Thus the $M2$ polyhedron occupied by the ferrous ion is also affected by the Fe/(Fe + Ca) ratio in the rest of the structure. Therefore, it is concluded that the $M2$ polyhedron obtained from X-ray refinement is not an artifact but represents the most probable polyhedral geometry for a given chemical composition.

Both the X-ray and the Mössbauer results indicate that a great change in the $M2$ polyhedral shape occurs at compositions between $Fs_{88}Wo_{12}$ and $Fs_{100}Wo_0$ (Fig. 3). The fact that the most rapid change occurs near the Fe-rich end of the solid solution is explained by the more severe effect expected for substitution of large Ca atoms into the small $M2$ polyhedron.

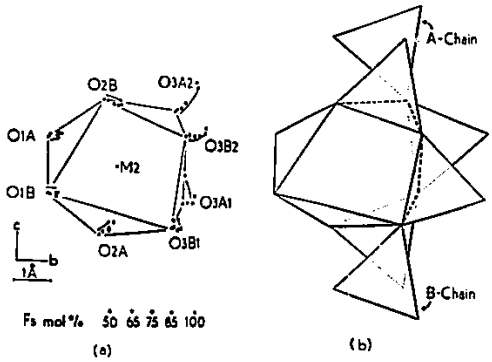

FIG. 2. (a) Variation of the oxygen positions around the $M2$ site in Ca-Fe clinopyroxenes. Arrows indicate shifts of the oxygen atoms *relative* to the $M2$ atom with Ca-Fe substitution; these may not represent actual shifts in the structure (see text, section on temperature factors, for discussion). Data for hedenbergite and clinoferrosilite are after Cameron *et al* (1973) and Burnham (1967), respectively. (b) Relation between the $M2$ site and the tetrahedral chains in $Fs_{88}Wo_{12}$. Note that positional changes of the O3 atoms shown in (a) result in rotations of the tetrahedral chains.

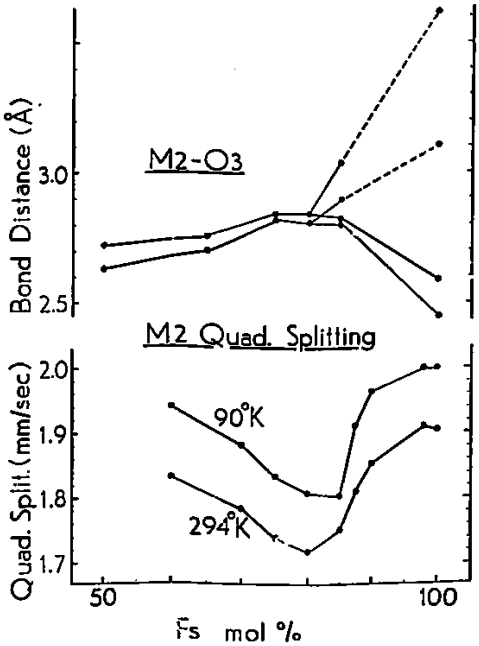

FIG. 3. Comparison of variations of the *M*2 quadrupole splitting (Dowty and Lindsley, 1973) and the *M*2–O3 interatomic distances with ferrosilite content in Ca-Fe clinopyroxenes. See Figure 1 for *M*2–O1 and *M*2–O2 distance variations. Note that both X-ray and Mössbauer studies indicate a sharp change in *M*2 polyhedral shape between the compositions $Fs_{65}Wo_{35}$ and $Fs_{100}Wo_0$.

Silicate Chains

Octahedral expansion affects the tetrahedal chains in three ways: (1) The silicate tetrahedra distort, (2) the tetrahedral chain angles change, and (3) the degree of out-of-plane tilting of the basal faces of the tetrahedra vary (Cameron *et al*, 1973). Details of these changes associated with Ca-Fe substitution are discussed below.

Tetrahedron. Interatomic distances and angles for the silicate tetrahedra are given in Table 6. The Si–O3 (bridging oxygen) bond is the longest of the Si–O bonds, and of the two nonbridging oxygens, the Si–O2 distance is shorter than the Si–O1. The angle O1–Si–O2, 114°–119°, is larger than the ideal tetrahedral angle, 109.46°.

The Si–O3 (bridging) bond distances (Fig. 4) decrease with replacement of Fe for Ca on the augite (Ca-rich) side, whereas the Si–O (nonbridging) bond distances increase. Variation on the pigeonite (Ca-poor) side, however, is not simple because there are two crystallographically distinct silicate chains. As the composition changes from $Fs_{50}Wo_{50}$ to $Fs_{75}Wo_{25}$, expansions of the Si–O1 and Si–O2 bonds are accompanied by contractions of *M*2–O1 and *M*2–O2, respectively. For the O3 atoms, contractions of the Si–O3 bonds are coupled with expansions of the *M*2–O3 bonds. The *M*1–O distances remain essentially constant with composition.

Qualitative discussions on bond distances can be developed by introducing a *bond strength*, defined by Zachariasen (1963). He assumes (1) that the bond strength is empirically related to the bond distance and (2) that the sum of bond strengths for each atom is set to its valence. Coupled changes in the Si–O and *M*2–O bond distances for the same oxygen atom are a natural consequence of the constant sum of the bond

TABLE 6. Interatomic Distances and Angles for Si Tetrahedra in Ca-Fe Clinopyroxenes

	$Fs_{65}Wo_{35}$	$Fs_{75}Wo_{25}$	$Fs_{80}Wo_{20}$	$Fs_{85}Wo_{15}$ A Chain	$Fs_{85}Wo_{15}$ B Chain
Distances (Å)					
Si–O1	1.602(2)*	1.621(6)	1.614(3)	1.616(7)	1.620(7)
–O2	1.593(2)	1.601(7)	1.590(3)	1.589(11)	1.616(8)
–O3(1)	1.672(2)	1.657(7)	1.660(3)	1.642(8)	1.677(8)
–O3(2)	1.657(2)	1.667(7)	1.647(3)	1.630(7)	1.640(6)
Mean, Sbrw**	1.598	1.611	1.605	1.603	1.618
Mean, Br**	1.665	1.662	1.654	1.636	1.659
Mean of 4	1.631	1.637	1.629	1.619	1.638
Quad. Elong.***	1.0048	1.0044	1.0042	1.0016	1.0067
O1–O2	2.728(3)	2.747(7)	2.737(4)	2.694(9)	2.783(9)
O1–O3(1)	2.678(3)	2.671(8)	2.668(5)	2.643(10)	2.672(11)
O1–O3(2)	2.669(3)	2.681(9)	2.659(4)	2.630(9)	2.666(9)
O2–O3(1)	2.580(3)	2.574(9)	2.573(5)	2.601(14)	2.565(13)
O2–O3(2)	2.655(3)	2.676(10)	2.648(5)	2.636(11)	2.652(10)
O3(1)–O3(2)	2.64.(1)	2.664(2)	2.659(2)	2.654(2)	2.688(3)
Angles (deg.)					
O1–Si–O2	117.2(1)	117.0(4)	117.0(2)	114.4(6)	118.7(6)
O1–Si–O3(1)	109.7(1)	109.2(3)	109.2(2)	108.4(4)	108.3(4)
O1–Si–O3(2)	109.9(1)	109.2(3)	109.2(2)	108.2(4)	109.7(4)
O2–Si–O3(1)	106.4(1)	106.4(4)	106.4(2)	107.3(5)	107.3(5)
O2–Si–O3(2)	109.5(1)	110.0(4)	109.4(2)	109.9(4)	109.1(4)
O3(1)–Si–O3(2)	105.3(1)	106.6(3)	107.1(1)	108.4(3)	108.2(3)
Ang. Var. (deg.^{2})†	20.7	18.4	17.9	6.9	28.2
O3–O3–O3††	162.5(2)	159.8(5)	159.5(3)	164.2(8)	156.0(7)
Si–O3–Si	136.5(1)	136.6(5)	136.8(2)	140.9(5)	135.5(5)
Out-of-plane tilting†††	3.7	4.5	4.7	4.2	5.8
Tetrahedral Volume (Å^3)					
	2.214	2.233	2.206	2.173	2.236

*Parenthesized figures represent the estimated standard deviation (esd) in terms of least units cited for the value to their immediate left, thus for 1.602(2) read 1.602 ± 0.002.

**Sbr = nonbridging oxygen atoms (O1 and O2), and
Br = bridging oxygen atom (O3).

***Tetrahedral quadratic elongation (Robinson *et al*., 1971) defined by $\sum_{i=1}^{4} (\ell_i/\ell_o)^2/4$, where ℓ_o is the center-to-vertex distance for an ideal tetrahedron whose volume is equal to the observed tetrahedron.

†Tetrahedral angle variance (Robinson *et al*., 1971) defined by $\sum_{i=1}^{6} (\theta_i - 109.47°)^2/5$.

††Tetrahedral chain angle. All chains listed here are O rotation (Thompson, 1970).

†††Angle between (100) and the basal face, O2–O3–O3, of a tetrahedron.

strengths. When the strength of one bond increases, that of another must decrease to maintain the sum constant. Because only three cations are coordinated to the O2 atom, the bond strengths for Si–O2, *M*1–O2, and *M*2–O2 are larger (thus shorter in length) than any other corresponding bonds for the O1 and O3 oxygens.

Tetrahedral Chain Angle. The tetrahedral chain angle, O3–O3–O3, has been shown to vary with chemical composition, particularly with Ca content, and also with temperature (Clark *et al*, 1969; Brown *et al*, 1972; Smyth and Burnham, 1972; Cameron *et al*, 1973). Proper attention must be given, however, not only to angles but also to the rotation direction with respect to the octahedra (Thompson, 1970; Papike *et al*, 1973). Overlooking the difference in the rotation sense, the chain in augites is often compared with the *A* chain in pigeonites on the basis of the apparent similarity of the tetrahedral chain angle, which is 165° for hedenbergite (Cameron *et al*, 1973) and 167° for the *A* chain in clinoferrosilite (Burnham, 1967). The sense of rotation is, however, reversed in these chains.

The variation of the tetrahedral chain angles with composition is plotted in Figure 5. As the effective size of *M*2 decreases by substitution of Fe for Ca, the chain becomes more kinked, from 165° in $Fs_{50}Wo_{50}$ to 159° in $Fs_{80}Wo_{20}$. The relation between the *M*2 site and the tetrahedral chains can be visualized using Figure 2: a vector connecting O3*B*1 and O3*B*2 can be seen to rotate clockwise when the composition changes from $Fs_{50}Wo_{50}$ to $Fs_{80}Wo_{20}$, and this rotation results in a decrease in the O3–O3–O3 angle. As the size of *M*2 decreases further from $Fs_{80}Wo_{20}$, the chains on opposite sides of each *M*2 polyhedron become crystallographically distinct. The *B* chain becomes increasingly kinked, whereas the *A* chain becomes extended and reverses its rotation direction between $Fs_{85}Wo_{15}$ and $Fs_{100}Wo_0$. Thus in $Fs_{100}Wo_0$ the *A* chain is "S-rotated" (Thompson, 1970) and the *B* chain is "O-rotated."

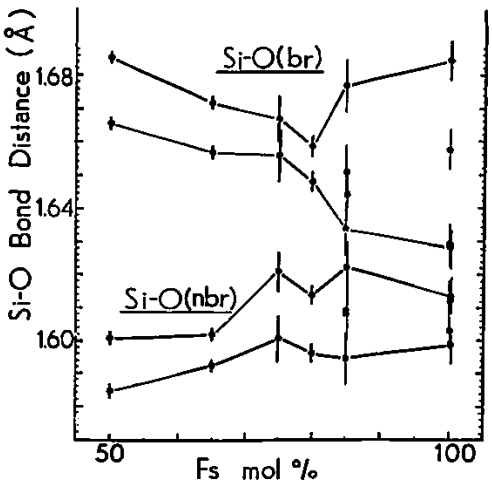

FIG. 4. Variation of Si-O interatomic distances with ferrosilite content in Ca-Fe clinopyroxenes. Error bars represent ±1 standard deviation. O(br) denotes the bridging oxygen atom, O3; O(nbr) denotes the nonbridging oxygen atoms, O1 and O2. Distances in hedenbergite and clinoferrosilite are after Cameron *et al* (1973) and Burnham (1967), respectively.

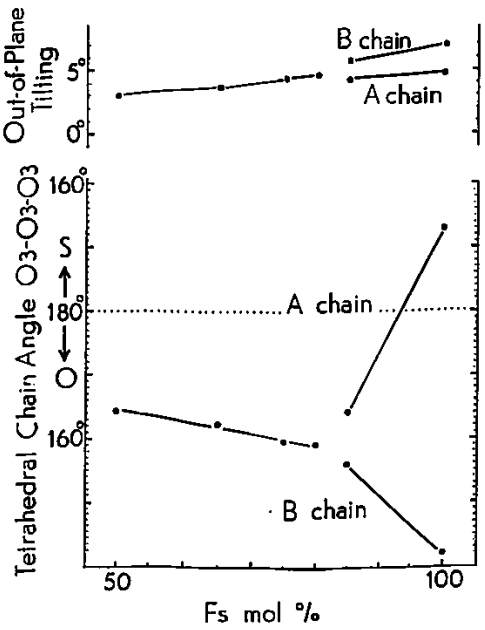

FIG. 5. Variation of the tetrahedral chain angle, O3–O3–O3, and the out-of-plane tilting of the basal triangle, defined by O2, O3, and O3, with the ferrosilite component in Ca-Fe clinopyroxenes. Angles for hedenbergite and clinoferrosilite were computed from the atomic coordinates given by Cameron *et al* (1973) and Burnham (1967), respectively. Standard errors are smaller than the radii of circles.

Out-of-Plane Tilting of the Basal Face of the Tetrahedron. The out-of-plane tilting of the basal face of the tetrahedron, which is defined as the angle between (100) and the basal face,

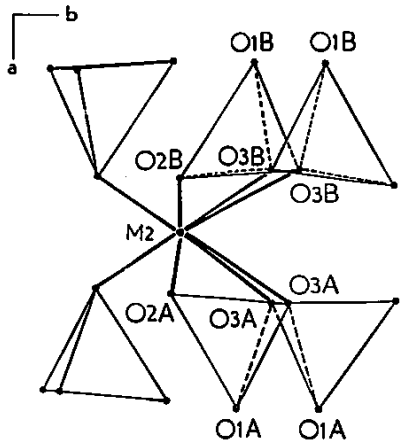

FIG. 6. A portion of the $Fs_{85}Wo_{15}$ structure showing the relation between the *M*2 site and the out-of-plane tilting of the basal face of the tetrahedron. The O2 atoms shift slightly toward *M*2 and away from the (100) plane, passing through the O3 atoms. As a result, the basal face of the tetrahedron tilts a few degrees with respect to (100). Out-of-plane tilting increases when the effective ionic size of *M*2 decreases, as would be expected from shortening of *M*2–O2 bonds.

O2–O3–O3′, of the tetrahedron, provides another measure to describe the silicate tetrahedral chain configuration. The direction of the observed tilting is such that the O1 and O2 atoms in the same tetrahedron are on opposite sides of the (100) plane containing the O3 atoms (Fig. 6). As exhibited in Figure 5 and Table 5, the out-of-plane tilting generally tends to increase when the composition changes from hedenbergite to ferrosilite. This increased tilting is a direct response of the tetrahedral chain to the changes in the *M*2 polyhedron. When the composition changes from $Fs_{50}Wo_{50}$ to $Fs_{80}Wo_{20}$ (Fig. 1), the *M*2–O2 distances decrease but *M*2–O3 distances increase. These changes in the *M*2–O distances will result in an increase in the out-of-plane tilting angle (Fig. 6). In the pigeonite region the tilting is larger for the *B* chain than for the *A* chain, reflecting the fact that *M*2–O2*B* < *M*2–O2*A* and *M*2–O3*B*1 > *M*2–O3*A*1 (Fig. 1).

There is a correlation between the tilting and the tetrahedral *B* chain angle (Fig. 5)—the more kinked the chain angle, the greater the out-of-plane tilting. This relationship may be explained by simple geometrical arguments. The kinking of the chain results in an increase in the offset of O3 atom pairs parallel to *b* (Fig. 2b). However, these changes have very little effect on the O1–O1 distance, which varies only from 3.088 Å in $Fs_{50}Wo_{50}$ to 3.040 Å in $Fs_{100}Wo_0$ as the chain angle decreases from 164.5° to 142°; therefore, the relative position of O1 is very nearly fixed. The only means of kinking the chain without moving O1 results in the movement of the O2 atom in such a manner that the out-of-plane tilting increases (Fig. 6).

Temperature Factors

The variation of isotropic temperature factors with composition (Fig. 7) falls into two groups: one (*M*2, O2, and O3) has a marked peak in the middle of the solid solution, whereas the other (*M*1, Si, and O1) is relatively flat. These differences in behavior can be explained by the effects of positional disorder due to multiple occupancy of the *M*2 site. Because the ionic radii of the Ca and Fe atoms are considerably

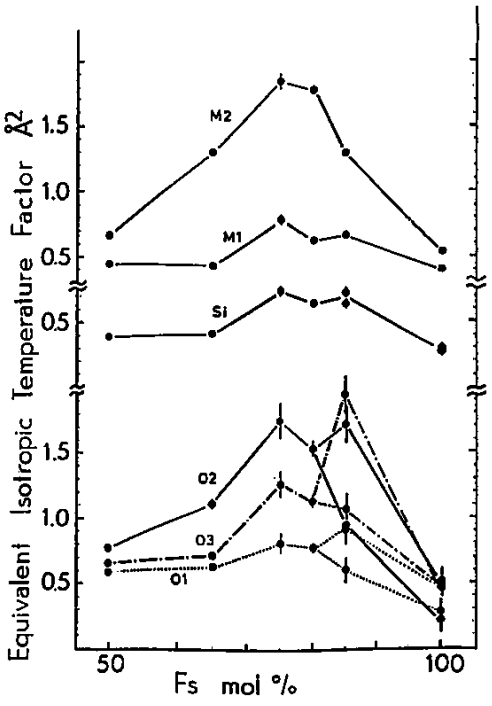

FIG. 7. Variation of equivalent isotropic temperature factors with ferrosilite content in Ca-Fe clinopyroxenes. Error bars represent ±1 standard deviation (if not shown, the standard deviation is smaller than the radii of circles). Data for hedenbergite and clinoferrosilite are after Cameron *et al* (1973) and Burnham (1967), respectively.

different, one might expect a positional fluctuation, which results from variation of the atomic positions (in terms of fractional coordinates of the unit-cell translations) from one unit cell to another. The effects of positional disorder may be significant, especially for the multiple occupancy sites.

In the clinopyroxenes under study, the *M*2 site shows its largest apparent temperature factor in the middle of the solid solution (Fig. 7), as is expected from its multiple occupancy by Ca and Fe atoms. The O2 and O3 atoms also exhibit large apparent temperature factors for intermediate compositions. This effect can be related to disorder of the tetrahedral chain rotation, as will be discussed below. In contrast *M*1 and Si, which are not directly linked to *M*2, show less significant effects of positional disorder. Interestingly, the positional disorder of the apical oxygen O1, although it is coordinated to *M*2, is the smallest among the oxygen atoms, indicating that the position of O1 is relatively well localized in the unit cell.

Some of the thermal vibration ellipsoids given in Table 7 show abnormally large anisotropy, which may be explained by positional disorder. The apparent thermal vibration ellipsoids for the atoms in the *M*2 polyhedron are shown in Figure 8. *M*2, for example, has the longest ellipsoid axis parallel to the *b* axis, except in hedenbergite, in which the longest axis is normal to the *b* axis. The thermal vibration ellipsoid in hedenbergite presumably represents

TABLE 7. Magnitudes and Orientations of the Principal Axes of Thermal Vibration Ellipsoids in Ca-Fe Clinopyroxenes

	Ellipsoid axis, r_i	r.m.s. amplitude (Å)	Angle (deg.) of r_i with a	b	c	r.m.s. amplitude (Å)	Angle (deg.) of r_i with a	b	c	r.m.s. amplitude (Å)	Angle (deg.) of r_i with a	b	c
			M1				M2				Si		
$Fe_{65}Wo_{35}$	1	0.066(2)*	90	0	90	0.078(2)	76(2)	90	30(2)	0.058(3)	114(7)	62(8)	30(6)
	2	0.069(2)	78(4)	90	177(4)	0.113(1)	166(2)	90	60(2)	0.070(3)	129(8)	140(8)	73(8)
	3	0.087(1)	12(4)	90	93(4)	0.175(1)	90	0	90	0.086(2)	49(5)	116(5)	66(4)
$Fe_{75}Wo_{25}$	1	0.092(5)	8(12)	90	98(12)	0.092(6)	49(5)	90	58(5)	0.083(6)	14(43)	76(48)	112(9)
	2	0.101(4)	90	0	90	0.142(5)	41(5)	90	148(5)	0.090(6)	76(47)	166(48)	96(22)
	3	0.109(5)	98(12)	90	8(12)	0.204(4)	90	0	90	0.116(5)	84(7)	90(14)	23(7)
$Fe_{80}Wo_{20}$	1	0.073(2)	139(18)	90	115(18)	0.100(2)	170(6)	90	83(6)	0.057(3)	139(9)	83(6)	114(8)
	2	0.080(2)	90	0	90	0.118(2)	109(6)	90	145(6)	0.080(3)	94(6)	161(3)	106(5)
	3	0.112(2)	109(5)	90	3(5)	0.209(2)	90	0	90	0.122(2)	110(5)	106(3)	17(3)
										Si A			
$Fe_{85}Wo_{15}$	1	0.086(4)	23(15)	112(24)	114(30)	0.084(2)	50(3)	92(2)	58(3)	0.070(7)	14(8)	103(10)	101(9)
	2	0.091(4)	87(34)	63(17)	149(26)	0.118(2)	41(3)	85(2)	147(3)	0.096(7)	92(12)	124(13)	141(12)
	3	0.099(5)	67(12)	36(13)	72(18)	0.185(2)	93(2)	5(2)	85(2)	0.117(6)	104(7)	143(12)	53(12)
										Si B			
										0.063(10)	57(11)	34(10)	96(13)
										0.087(6)	52(13)	111(13)	149(10)
										0.111(7)	56(8)	115(8)	59(10)
			O1				O2				O3		
$Fe_{65}Wo_{35}$	1	0.083(6)	87(102)**	133(154)	46(186)	0.080(6)	71(8)	25(3)	79(9)	0.069(7)	99(12)	66(5)	24(5)
	2	0.084(6)	58(18)	127(160)	136(186)	0.105(5)	41(6)	94(9)	146(5)	0.090(5)	169(11)	89(8)	85(12)
	3	0.100(4)	33(14)	65(13)	84(13)	0.156(4)	55(4)	115(3)	58(4)	0.117(5)	85(8)	24(5)	114(5)
$Fe_{75}Wo_{25}$	1	0.061(27)	127(21)	48(14)	53(10)	0.092(17)	50(35)	40(35)	101(14)	0.086(16)	27(26)	112(12)	119(26)
	2	0.098(17)	143(21)	120(20)	95(17)	0.110(15)	139(35)	50(35)	70(9)	0.107(13)	112(29)	108(15)	137(23)
	3	0.135(15)	90(15)	124(11)	37(9)	0.215(12)	83(5)	95(5)	24(6)	0.171(11)	75(7)	20(8)	118(8)
$Fe_{80}Wo_{20}$	1	0.076(7)	115(17)	99(13)	108(16)	0.072(8)	131(29)	53(32)	104(11)	0.065(9)	134(13)	101(5)	118(12)
	2	0.101(6)	80(15)	167(18)	85(19)	0.094(7)	119(24)	125(14)	120(16)	0.111(6)	56(13)	126(6)	136(9)
	3	0.117(5)	96(11)	88(28)	10(12)	0.210(5)	115(7)	111(3)	24(4)	0.164(5)	90(3)	147(4)	59(4)
$Fe_{85}Wo_{15}$ A chain	1	0.054(22)	52(13)	92(32)	56(13)	0.110(13)	146(15)	74(28)	45(9)	0.032(45)	35(12)	104(7)	76(9)
	2	0.093(17)	99(49)	169(56)	82(48)	0.133(15)	105(25)	164(28)	79(21)	0.108(13)	56(12)	59(5)	142(6)
	3	0.106(12)	140(19)	79(56)	35(19)	0.187(13)	61(7)	92(12)	47(7)	0.248(11)	98(3)	35(3)	55(3)
	1	0.084(15)	153(24)	78(22)	49(18)	---***	51(15)	43(12)	87(10)	0.051(30)	143(9)	104(6)	40(8)
B chain	2	0.113(20)	116(25)	126(43)	120(35)	0.106(21)	40(15)	124(13)	120(10)	0.129(14)	125(10)	86(19)	127(10)
	3	0.128(17)	84(26)	141(41)	56(28)	0.166(11)	86(8)	112(7)	30(9)	0.157(12)	99(13)	15(8)	76(13)

*Parenthesized figures represent the estimated standard deviation (esd) in terms of least units cited for the value to their immediate left, thus for 0.066(2) read 0.066 ± 0.002.
**Orientation of axis is indeterminate because the ellipsoid is essentially uniaxial.
***The corresponding eigen value is close to zero but negative.

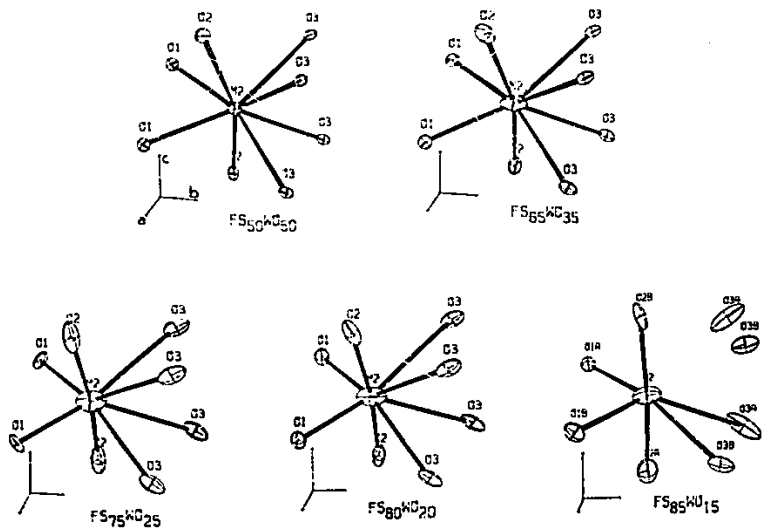

FIG. 8. Apparent thermal vibration ellipsoids for atoms in the $M2$ polyhedron in Ca-Fe clinopyroxenes. The ellipsoids represent 70 percent probability surfaces (1.92 times the r.m.s. amplitude). Ellipsoids for hedenbergite were calculated from data given by Veblen (1969). For the O2*B* site in $Fs_{85}Wo_{15}$, β_{12} is decreased by 2 standard deviations to obtain a positive definite tensor. Drawing produced by ORTEP (Johnson, 1965).

primarily intrinsic vibrations, whereas those in intermediate compositions include significant effects of positional disorder. As for the $M2$ displacement, this study suggests the same interpretation reached by Takeda (1972). Since O1 shows relatively small changes in ellipsoid shape throughout the solid solution, it seems reasonable to conclude that as the composition becomes more iron-rich, the mean position of $M2$ shifts toward O1 rather than the other way.

In intermediate compositions the longest ellipsoid axis for the O2 atom tends to orient parallel to the bond direction of $M2$–O2 (Fig. 9a). Since $M2$–O2 is the shortest bond in the $M2$ polyhedron, the multiple occupancy of the Ca and Fe atoms in $M2$ may produce significant disorder of O2 along the bond direction.

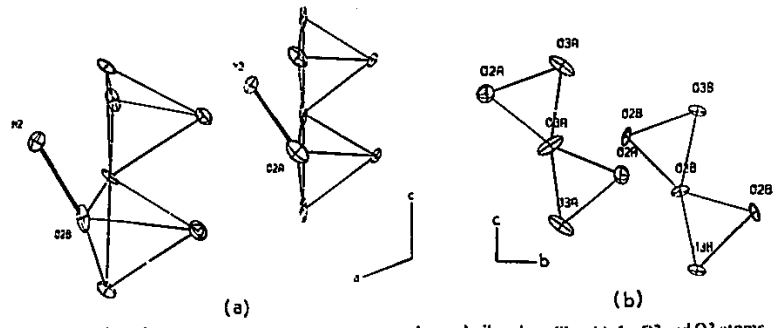

FIG. 9. Explanation of the abnormally large apparent thermal vibration ellipsoids for O2 and O3 atoms in $Fs_{85}Wo_{15}$. See text. Ellipsoids shown are 70 percent probability surfaces (1.92 times the r.m.s. amplitude). For the O2*B* atom, β_{12} is decreased by 2 standard deviations to obtain a positive definite tensor. Drawing produced by ORTEP (Johnson, 1965).

The large apparent thermal vibration ellipsoid for the O3 atoms in the intermediate compositions can be interpreted as positional disorder associated with tetrahedral chain rotation (Fig. 9b). As previously shown (Fig. 2) the change in size of the $M2$ cation causes a rotation of the tetrahedral chains. The rotation angle of the individual chains may be slightly different from the average chain angle, and the resulting positional fluctuation will appear as large apparent vibrations of O3 in (100), the approximate plane of the rotation, and along a bisecting direction of the basal faces of the two tetrahedra bridged by O3. O1 and Si, however, are close to the rotation axis and thus are not affected by this rotation.

Conclusions

As composition changes on the hedenbergite-ferrosilite join, the polyhedral volume and bond distances of the $M1$ site do not change appreciably, except for a slight distortion of the polyhedron. Such lack of change in $M1$ confirms that few, if any, Ca atoms can occupy $M1$ sites in the Ca-Fe clinopyroxenes studied.

In the $M2$ coordination polyhedron the $M2$–O1 and $M2$–O2 distances and the polyhedral volume decrease when the composition changes from hedenbergite to ferrosilite. The $M2$–O3 distances exhibit a sharp change between the compositions $Fs_{85}Wo_{15}$ and $Fs_{100}Wo_0$.

The decrease in the average size of the $M2$ atom causes kinking of the tetrahedral B chain. Extension and reversal of rotation sense of the A chain occur between the compositions $Fs_{85}Wo_{15}$ and $Fs_{100}Wo_0$. The decrease in $M2$ cation size causes an increase in the out-of-plane tilting of the basal face of the tetrahedron.

The large temperature factors found for the $M2$, O2, and O3 atoms in intermediate compositions of the Ca-Fe clinopyroxenes can be explained by the effect of atomic positional disorder due to multiple occupancy in $M2$.

Together with the crystal structures of the end-member clinopyroxenes at high temperatures (Cameron *et al*, 1973), the results of the present study could provide a basis for future studies of the crystal structures of intermediate clinopyroxenes at high temperature. These studies, which will undoubtedly have mineralogical significance for a better understanding of crystallization and exsolution in natural pyroxenes, are also necessary for relating the crystal structures to the experimentally determined phase diagram.

Acknowledgments

We thank Dr. D. H. Lindsley for supplying the synthetic pyroxene crystals, and Drs. H. S. Yoder, Jr., G. E. Brown, C. T. Prewitt, and S. Sueno for their many helpful comments and suggestions on the manuscript. The present study is based partly on the first author's Ph.D. dissertation (Ohashi, 1973), accepted by the Department of Geological Sciences, Harvard University. That part of the study was supported by the National Science Foundation grant GA-12852 to C.W.B. The remainder of the work was performed at the Geophysical Laboratory, Carnegie Institution of Washington. Thanks are due Miss D. M. Thomas for editing and typing the manuscript.

References

Bowen, N. L., J. F. Schairer, and E. Posnjak (1933) The system CaO-FeO-SiO_2. *Am. J. Sci.* **26**, 193–284.

Brown, G. E., C. T. Prewitt, J. J. Papike, and S. Sueno (1972) A comparison of the structures of low and high pigeonite. *J. Geophys. Res.* **77**, 5778–5789.

Burnham, C. W. (1962) Lattice constant refinement. *Carnegie Inst. Wash. Year Book*, **61**, 132–135.

——— (1966) Computation of absorption correction and the significance of end effect. *Am. Mineral.* **51**, 159–167.

——— (1967) Ferrosilite. *Carnegie Inst. Wash. Year Book*, **65**, 285–290.

———, J. R. Clark, J. J. Papike, and C. T. Prewitt (1967) A proposed crystallographic nomenclature for clinopyroxene structures. *Z. Kristallogr.* **125**, 109–119.

Cameron, M., S. Sueno, C. T. Prewitt, and J. J. Papike (1973) High-temperature crystal chemistry of acmite, diopside, hedenbergite, jadeite, spodumene, and ureyite. *Am. Mineral.* **58**, 594–618.

Clark, J. R., D. E. Appleman, and J. J. Papike (1969) Crystal-chemical characterization of clinopyroxenes based on eight new structure refinements. *Mineral. Soc. Am. Spec. Pap.* **2**, 31–50.

Cromer, D. T. (1965) Anomalous dispersion corrections computed from self-consistent field relativistic Dirac-Slater wave functions. *Acta Crystallogr.* **18**, 17–23.

———, and J. B. Mann (1968) X-ray scattering factors computed from numerical Hartree-Fock wave functions. *Acta Crystallogr.* **24**, 321–324.

Dowty, E., and D. H. Lindsley (1973) Mössbauer spectra of synthetic hedenbergite-ferrosilite pyroxenes. *Am. Mineral.* **58**, 850–868.

Gabe, E. J., G. E. Alexander, and R. H. Goodman (1970) The Mines Branch on-line single-crystal diffractometer. *Mineral Sci. Div., Dep. Energy, Mines Resources, Canada, Internal Rep.* MS71-54.

Güven, N. (1969) Nature of the coordination polyhedra around $M2$ cations in pigeonite. *Contrib. Mineral. Petrol.* **24**, 268–274.

Hamilton, W. C. (1959) On the isotropic temperature factor equivalent to a given anisotropic temperature factor. *Acta Crystallogr.* **12**, 609–610.

Johnson, C. K. (1965) Ortep, a Fortran thermal ellipsoid plot program for crystal structure illustrations. *U.S. Nat. Tech. Inform. Serv.* ORNL-3794.

Lindsley, D. H., and J. L. Munoz (1969) Subsolidus relations along the join hedenbergite-ferrosilite. *Am. J. Sci.* **267A**, 295–324.

Morimoto, N., D. Appleman, and H. T. Evans (1960) The

crystal structures of clinoenstatite and pigeonite. *Z. Kristallogr.* **114**, 120–147.

———, AND N. GÜVEN (1970) Refinement of the crystal structure of pigeonite. *Am. Mineral.* **55**, 1195–1209.

OHASHI, Y. (1973) *High Temperature Structural Crystallography of Synthetic Clinopyroxene*, (Ca,Fe)SiO_3. Ph.D. Thesis, Harvard University.

———, AND C. W. BURNHAM (1973) Clinopyroxene lattice deformations: the roles of chemical substitution and temperature. *Am. Mineral.* **58**, 843–849.

PAPIKE, J. J., C. T. PREWITT, S. SUENO, AND M. CAMERON (1973) Pyroxenes: comparisons of real and ideal structural topologies. *Z. Kristallogr.* **138**, 254–273.

ROBINSON, K., G. V. GIBBS, AND P. H. RIBBE (1971) Quadratic elongation: a quantitative measure of distortion in coordination polyhedra. *Science*, **172**, 567–570.

SMYTH, J. R., AND C. W. BURNHAM (1972) The crystal structures of high and low clinohypersthene. *Earth Planet. Sci. Lett.* **14**, 183–189.

TAKEDA, H. (1972) The crystallography of some aluminous orthopyroxenes of high pressure origin. *J. Geophys. Res.* **77**, 5798–5811.

THOMPSON, J. B., JR. (1970) Geometrical possibilities for amphibole structures. *Am. Mineral.* **55**, 292–293.

VEBLEN, D. R. (1969) *The Crystal Structures of Hedenbergite and Ferrosilite*. A. B. Thesis, Harvard University.

ZACHARIASEN, W. H. (1963) The crystal structure of monoclinic metaboric acid. *Acta Crystallogr.* **16**, 385–389.

——— (1968) Experimental tests of the general formula for the integrated intensity of a real crystal. *Acta Crystallogr.* **A24**, 212–216.

Manuscript received, September 16, 1974; accepted for publication, December 19, 1974.

Fs65-Wp35

H OBS CALC H OBS CALC H OBS CALC H OBS CALC

H	OBS	CALC
H 0 0		
-14	755	747
-10	822	829
-8	1009	1046
-6	1274*	1337
-4	533*	627
-2	741*	662
0	0	4952
2	744*	662
4	538*	627
6	1305	1337
8	1037	1046
10	851	829
14	787	747
H 0 2		
-14	747	732
-12	128	107
-10	978	971
-8	604	594
-6	1386	1436
-4	1458*	1602
-2	106	138
2	1372	1421
4	1402*	1476
6	300	291
8	677	667
12	121	110
H 0 4		
-14	830	806
-12	350	336
-10	696	690
-8	267	251
-6	1344	1387
-4	1155	1155
-2	218	219
0	1360*	1430
2	553	551
4	1135	1156
6	461	463
8	448	434
10	616	600
H 0 6		
-12	336	317
-10	1003	991
-8	37	38
-6	608	608
-4	1026	1034
-2	505	517
0	609	630
2	263	259
4	1005	1025
6	288	294
H 0 8		
-8	256	237
-6	493	495
-4	367	365
-2	473	502
0	687	714
H 1 0		
-15	68	48
-11	363	368
-9	204	188
-7	689	694
-5	311	313
-3	1185	1204
3	1210	1204
5	314	313
7	701	694
9	205	188
11	375	368
13	46	42
15	53	48
H 1 1		
-15	79	80
-11	188	168
-9	45	65
-7	272	278
-5	257	241
-3	710	702
-1	108	81
1	61	36
3	570	576
5	168	157
7	268	269
9	112	104
11	209	208
H 1 2		
-15	93	81
-13	379	366
-11	90	103
-9	95	95
-7	1212	1214
-5	101	70
-3	317	296
-1	453*	387
1	959	936
3	550	547
5	218	218
7	763	759
9	48	58
11	328	307
13	191	181
H 1 3		
-13	44	35
-7	353	334
-5	394	374
-3	519	517
-1	71	64
1	50	42
3	253	251
H 1 4		
-13	290	281
-11	297	291
-9	33	21
-7	505	495
-5	94	78
-3	1008	970
-1	253	253
1	240	239
3	762	771
5	32	33
7	288	291
11	388	369
H 1 5		
-13	109	109
-9	43	43
-7	294	287
-5	210	221
-3	306	298
-1	38	24
1	117	107
3	114	104
7	258	256
9	122	105
H 1 6		
-13	413	402
-11	146	143
-7	503	497
-5	78	85
-3	567	541
-1	80	79
1	234	239
3	168	168
5	110	107
7	411	414
H 1 7		
-7	183	192
-5	146	152
-3	223	214
1	102	113
H 1 8		
-6	81	80
-4	200	187
-2	131	135
0	129	129
H 2 0		
-14	50	53
-12	170	159
-8	223	221
-6	57	69
H 2 1		
-14	86	64
-12	443	438
-10	193	205
-8	621	633
-6	674	706
-4	1016	1047
-2	1687*	1460
0	98	47
2	1442*	1537
4	699	708
6	879	905
8	653	644
10	79	92
12	676	654
14	185	167
H 2 2		
-13	154	152
-9	81	89
-7	247	261
-5	255	254
-3	187	137
-1	507	492
1	391	390
3	120	91
5	233	242
7	195	210
9	82	86
13	169	155
H 2 3		
-11	584	578
-9	1026	1033
-7	69	52
-5	1073	1099
-3	694	658
-1	1574	1562
1	705	682
3	268	251
5	1165	1178
7	370	355
9	694	676
11	130	114
H 2 4		
-14	133	132
-12	248	242
-10	41	31
-8	82	77
-4	333	321
-2	250	232
0	286	289
2	505	511
4	69	67
8	144	130
10	154	143
H 2 5		
-14	87	88
-12	531	547
-10	102	111
-8	829	834
-6	371	376
-4	356	349
-2	813	799
0	328	336
2	891	911
6	500	506
8	467	461
H 2 6		
-12	183	185
-10	128	136
-8	210	200
-6	89	89
-4	48	17
-2	156	155
0	53	37
2	241	226
4	67	54
6	160	173
H 2 7		
-10	45	28
-8	639	663
-6	292	295
-4	355	336
-2	477	466
0	182	184
2	646	668
4	122	127
H 2 8		
-8	86	85
-6	81	80
-4	200	187
-2	131	135
0	129	129
H 3 0		
-11	143	143
-9	237	253
-7	123	108
-5	273	291
H 3 1		
-15	396	394
-13	343	333
-11	578	560
-9	959	975
-7	130	133
-5	1462*	1541
-3	1388	1431
-1	1432	1446
1	336	371
3	801	786
5	1841*	1979
7	110	98
9	639	632
11	423	402
13	515	481
H 3 2		
-15	84	88
-13	154	152
-9	81	89
-7	247	261
-5	255	254
-3	187	137
-1	507	492
1	391	390
3	120	91
5	233	242
7	195	210
9	82	86
13	169	155
H 3 3		
-15	412	413
-13	159	159
-11	584	578
-9	1026	1033
-7	69	52
-5	1073	1099
-3	694	658
-1	1574	1562
1	705	682
3	268	251
5	1165	1178
7	370	355
9	694	676
11	130	114
H 3 4		
-15	72	65
-13	41	32
-11	159	157
-9	183	194
-7	103	86
-5	241	234
-3	245	257
-1	76	81
1	36	55
3	249	266
5	157	154
7	41	34
9	199	193
11	90	91
H 3 5		
-13	69	73
-11	313	296
-9	877	892
-7	363	355
-5	761	737
-3	126	114
-1	1214	1194
1	593	593
3	237	229
5	697	700
7	269	253
9	605	606
H 3 6		
-13	107	99
-9	57	59
-7	173	166
-5	132	130
-3	94	80
-1	244	241
1	147	142
5	129	132
7	134	128
H 3 7		
-11	261	260
-9	394	405
-7	398	388
-5	826	801
-3	69	70
-1	630	626
1	524	529
3	348	360
H 3 8		
-5	139	132
-3	114	112
H 4 0		
-14	101	109
-12	146	127
-10	505	512
-8	71	54
-6	110	85
-4	745	742
-2	31	15
0	239	252
2	37	15
4	725	742
6	91	85
8	67	54
10	519	512
12	141	127
14	100	109
H 4 1		
-14	174	165
-12	415	407
-10	198	194
-8	68	55
-6	100	75
-4	135	112
-2	484	449
0	638	652
2	597	556
4	150	162
6	156	141
8	200	183
10	234	235
12	233	221
14	58	57
H 4 2		
-14	280	281
-12	159	143
-10	299	304
-8	77	80
-6	275	281
-4	182	180
-2	114	78
0	837	814
2	314	288
4	369	380
6	163	180
8	38	17
10	197	183
H 4 3		
-15	75	66
-11	70	59
-9	111	92
-7	110	100
-5	372	380
-3	280	262
-1	143	110
1	223	242
3	41	24
5	92	78
7	49	57
9	179	181
11	113	103
H 4 4		
-14	177	181
-12	165	156
-10	434	447
-8	76	59
-6	115	113
-4	354	347
-2	34	40
0	310	299
2	183	163
4	476	479
6	36	33
8	37	12
10	214	211
H 4 5		
-14	121	122
-12	243	250
-10	193	186
-8	295	291
-4	83	73
-2	204	189
0	131	140
2	376	380
4	321	311
6	88	83
8	133	132
H 4 6		
-10	220	190
-6	293	288
0	421	429
2	223	206
4	179	179
6	123	112
H 4 7		
-10	178	175
-8	302	304
-6	65	61
-4	48	21
-2	133	137
0	139	150
2	225	229
4	116	114
H 4 8		
-6	131	143
-4	112	112
H 5 0		
-13	399	402
-11	479	484
-9	373	363
-7	1381	1424
-5	159	169
-3	1014	1018
-1	1358	1371
1	1290*	1371
3	973	1018
5	149	169
7	1371	1424
9	382	363
11	407	484
13	411	402
H 5 1		
-11	145	128
-9	101	109
-5	39	47
-3	281	244
-1	260	262
1	52	59
3	268	250
5	170	186
7	81	62
9	53	49
11	50	41
H 5 2		
-13	437	431
-11	485	496
-9	351	359
-7	1203	1226
-5	415	414
-3	1290	1317
-1	510	505
1	1064	1058
3	1378	1433
5	161	163
7	823	823
9	390	389
11	667	667
H 5 3		
-13	75	66
-11	70	59
-9	111	92
-7	110	100
-5	372	380
-3	280	262
-1	143	110
1	223	242
3	41	24
5	92	78
7	49	57
9	179	181
11	113	103
H 5 4		
-13	666	658
-11	389	395
-9	167	167
-7	1056	1090
-5	406	404
-3	1070	1027
-1	378	375
1	793	778
3	856	855
5	324	323
7	750	744
9	141	122
H 5 5		
-13	62	45
-9	78	79
-7	138	126
-5	111	105
-3	45	32
1	79	68
5	69	101
7	140	143
H 5 6		
-11	491	493
-9	320	317
-7	546	536
-5	254	246
-3	1094	1056
-1	222	211
1	428	424
3	629	637
5	357	352
H 5 7		
-7	81	96
-5	157	156
-3	77	73
H 6 0		
-12	178	175
-10	626	621
-8	409	402
-6	364	347
-4	520	488
-2	125	105
0	1502	1530
2	127	105
4	507	488
6	366	347
8	414	402
10	629	621
12	185	175
H 6 1		
-14	94	75
-10	151	149
-8	71	62
-6	192	194
-4	284	280
-2	194	177
0	340	336
2	147	154
4	122	123
8	158	153
10	149	139
12	81	73
H 6 2		
-14	592	577
-12	87	60
-10	343	345
-8	262	254
-6	891	883
-4	465	425
-2	348	347
0	1379	1387
2	330	308
4	521	496
6	159	153
8	345	332
10	532	514
H 6 3		
-14	139	125
-12	102	103
-10	175	168
-8	99	93
-6	52	44
-4	86	87
-2	137	142
0	256	238
2	129	125
4	284	275
6	110	91
10	137	117
H 6 4		
-12	104	94
-10	524	527
-8	137	131
-6	597	594
-4	811	777
-2	95	96
0	546	521
2	213	204
4	788	789
8	133	121
H 6 5		
-8	129	135
H 6 6		
-10	496	502
-8	105	112
-6	408	403
-4	460	447
-2	164	160
0	450	456
2	55	76
4	525	536
H 6 7		
-8	44	28
-6	45	40
-4	70	42
-2	124	114
0	95	99
2	58	51
H 7 0		
-13	44	35
-9	155	156
-7	370	377
-5	365	368
-3	92	76
-1	47	59
1	55	59
3	90	76
5	365	368
7	376	377
9	152	156
11	37	18
13	39	35
H 7 1		
-13	294	277
-11	253	250
-9	371	378
-7	72	71
-5	979	979
-3	121	85
-1	542	530
1	738	749
3	205	208
5	608	598
7	165	162
9	563	555
H 7 2		
-9	119	115
-7	255	262
-5	285	279
-3	291	274
-1	231	230
3	295	303
5	307	306
7	127	127
H 7 3		
-13	152	154
-11	217	216
-9	505	513
-7	72	80
-5	657	648
-3	149	154
-1	715	695
1	358	351
3	178	181
5	626	617
7	84	67
9	436	418
H 7 4		
-13	165	167
-11	40	30
-9	185	189
-7	302	299
-5	201	196
-3	171	166
-1	175	167
1	46	40
3	99	92
5	184	168
7	156	175
9	187	190
H 7 5		
-11	325	323
-9	299	293
-7	88	70
-5	716	698
-3	54	23
-1	428	409
1	401	394
3	253	247
5	274	276
7	99	91
H 7 6		
-9	59	58
-7	77	64
-5	172	168
-3	299	292
-1	192	183
1	61	52
3	98	97
H 7 7		
-7	110	95
-5	404	386
-3	114	107
-1	388	393

H	OBS	CALC
	H 7 7	
1	123	115
	H 8 0	
-12	68	45
-10	219	209
-8	55	28
-4	311	305
-2	119	109
2	118	109
4	308	305
6	30	5
10	222	209
12	68	45
	H 8 1	
-12	646	636
-10	216	216
-8	633	637
-6	405	407
-4	542	532
-2	1359	1365
0	39	40
2	840	834
4	561	576
6	774	774
8	405	391
10	94	104
12	699	682
	H 8 2	
-12	38	6
-10	152	141
-8	88	77
-6	54	47
-4	116	106
-2	169	144
0	179	176
2	39	41
4	168	163
6	176	160
8	36	5
10	71	56
	H 8 3	
-12	674	678
-10	239	240
-8	612	619
-6	364	377
-4	475	469
-2	1001	970
0	249	252
2	903	896
4	130	129
6	632	633
8	584	578
10	118	109

H	OBS	CALC
	H 8 4	
-12	54	51
-10	165	163
-8	116	96
-4	109	96
-2	164	144
0	129	115
4	164	151
6	131	100
	H 8 5	
-2	802	790
0	288	286
2	656	658
4	134	133
6	508	500
	H 8 6	
-8	100	96
-6	144	123
-2	52	35
0	210	205
	H 8 7	
-4	356	341
-2	313	309
	H 9 0	
-11	115	111
-7	197	183
-5	85	90
-3	253	237
-1	36	20
1	30	20
3	248	237
5	87	90
7	201	183
11	114	111
	H 9 1	
-11	260	270
-9	245	259
-7	388	376
-5	690	710
-3	141	147
-1	188	186
1	113	123
3	65	70
5	592	605
7	187	166
9	254	275
11	40	18

H	OBS	CALC
	H 9 2	
-11	67	63
-9	68	48
-7	259	249
-5	91	87
-3	191	171
-1	116	105
1	134	119
5	81	74
7	224	209
9	55	62
	H 9 3	
-11	121	125
-9	517	545
-7	229	208
-5	214	224
-3	70	86
-1	630	634
1	76	56
3	183	164
5	581	606
7	59	44
9	158	171
	H 9 4	
-11	71	71
-7	171	152
-5	73	75
-3	247	231
-1	48	52
1	69	61
3	152	130
7	111	108
	H 9 5	
-9	282	305
-5	350	358
-3	266	238
-1	399	414
1	226	261
3	103	75
5	144	158
	H 9 6	
-7	152	152
-3	161	138
-1	50	28
1	111	99
	H 10 0	
-10	547	531
-8	286	277
-6	396	358
-4	642	624
-2	222	207
0	868	855
2	218	207

H	OBS	CALC
4	634	624
6	361	358
8	288	277
10	554	531
	H 10 1	
-10	54	75
-8	199	188
-4	48	61
-2	392	374
0	167	197
2	154	111
4	46	34
6	154	145
8	41	12
10	75	89
	H 10 2	
-10	558	551
-8	274	261
-6	417	406
-4	594	572
-2	255	235
0	770	740
2	182	173
4	696	676
6	286	271
8	230	225
	H 10 3	
-10	61	69
-8	79	63
-6	75	51
-4	59	39
-2	167	132
0	92	113
2	293	278
4	114	143
6	76	50
8	175	165
	H 10 4	
-10	468	466
-8	205	194
-6	477	459
-4	470	441
-2	246	227
0	670	633
2	126	111
4	587	563
6	282	269
	H 10 5	
-8	248	237
-6	75	76
-2	259	239
0	69	85

H	OBS	CALC
	H 10 5	
2	111	102
	H 10 6	
-4	356	336
-2	298	267
	H 11 0	
-9	163	187
-7	616	669
-5	125	82
-3	480	513
-1	374	412
1	374	412
3	472	513
5	130	82
7	620	669
9	161	187
	H 11 1	
-9	57	62
-7	140	106
-5	169	161
-3	48	68
-1	41	4
1	265	240
3	64	34
5	76	96
7	162	136
9	127	126
	H 11 2	
-9	70	83
-7	669	715
-3	446	484
-1	119	164
1	438	474
3	552	590
5	119	64
7	435	473
	H 11 3	
-9	39	37
-7	100	84
-5	56	28
-3	66	48
-1	69	63
1	93	55
3	78	52
5	79	72
	H 11 4	
-7	483	521
-5	156	145
-3	561	586
-1	38	43
1	266	303

H	OBS	CALC
	H 11 4	
3	476	520
5	103	120
	H 11 5	
-5	188	175
-3	51	30
-1	69	81
1	151	136
	H 12 0	
-8	130	136
-6	97	107
-4	62	78
-2	135	119
0	574	578
2	125	119
4	72	78
6	104	107
8	123	136
	H 12 1	
-8	209	160
-6	277	237
-4	220	181
-2	344*	273
0	82	37
2	495	444
4	98	54
6	210	169
8	296	263
	H 12 2	
-6	273	287
-4	129	133
-2	261	250
0	441	456
4	158	170
6	64	48
	H 12 3	
-8	345	315
-6	133	91
-4	159	108
-2	449	397
0	81	40
2	301	248
4	146	120
	H 12 4	
-6	257	262
-4	258	272
-2	200	177
0	203	207

H	OBS	CALC
	H 13 0	
-7	206	169
-3	280*	130
-1	127	68
1	124	68
3	202*	130
5	43	45
7	212	169
	H 13 1	
-7	186	122
-5	518	520
-3	174	196
-1	491	512
1	328	332
3	144	149
5	600	622
	H 13 2	
-7	191	148
-5	39	29
-3	223*	158
-1	89*	14
1	116	61
3	212	161
5	46	34
	H 13 3	
-5	587	611
-3	99	110
-1	402	411
1	394	408
3	189	199
	H 14 0	
0	202	179
	H 14 1	
-4	165*	241
-2	349*	425
0	211*	130
2	331*	416
	H 14 2	
-2	43	50
0	135	88

2. 218 207 0 69 85 1 266 303

MOORE BUSINESS FORM, INC. F 1410 PRINTED IN U.S.A.

FS75W025

H	OBS	CALC
H 0 0		
0	0	5000
2	867*	778
4	530*	592
6	1425	1381
8	972	1017
10	870	898
14	632	662
H 0 2		
-14	671	682
-10	946	949
-8	575	561
-6	1485	1489
-4	1635	1646
0	1904*	2037
2	1448	1467
4	1475	1471
6	445	409
8	517	517
10	1110	1108
H 0 4		
-14	728	720
-12	339	322
-10	697	652
-8	220	219
-6	1101*	1241
-4	872*	1148
0	1095*	1319
2	513	504
4	971	1012
6	539	578
8	295	316
10	562	566
H 0 6		
-12	280	256
-10	450	440
-6	321*	452
-4	633*	869
-2	310*	428
0	520*	595
4	787	751
6	371	360
H 0 7		
-8	239*	0
H 0 8		
2	782	807
4	283	279
6	636	619
8	540	523
12	401	402
H 1 0		
1	520*	447
3	1306	1286
5	288	268
7	695	692
9	234	251
11	259	305
H 1 1		
-11	165	148
-7	285	283
-5	182	181
-3	780	741
3	563	574
7	267*	324
H 1 2		
-13	424	410
-9	194*	25
-7	1231	1221
-3	267*	334
-1	418	459
1	872	894
3	627	630
5	249	215
7	728	724
11	243	219
13	206	233
H 1 3		
-7	382	345
-5	323	334
-3	407	448
-1	167	148
3	280	288
7	295	288
H 1 4		
-13	314	319
-11	247	269
-7	466	493
-3	890*	908
1	198	168
3	741	773
7	288	259
11	320	271
H 1 5		
-7	281	264
3	206	197
7	202	211
H 1 6		
-13	379	365
-7	378*	443
-3	300*	453
3	241	209
7	338	328

H	OBS	CALC
H 1 7		
-9	365*	40
-3	288*	188
H 1 8		
-9	250*	141
-3	448*	365
H 2 0		
0	193	211
2	790	774
4	258	261
8	319	316
H 2 1		
-12	753	774
-8	618	606
-6	593	579
-4	1029	987
-2	1841*	1734
0	151	144
2	1396	1394
4	691	682
6	727	725
8	628	650
12	576	576
H 2 2		
-12	272	278
-10	267	271
-8	390	347
-6	506	498
-4	140	115
-2	224*	258
0	445	426
2	553	558
4	151	131
6	287	292
8	342	333
12	217	194
H 2 3		
-12	578	576
-10	220	219
-8	846	851
-6	226	228
-4	407	415
-2	1430*	1519
0	218	252
2	782	807
4	283	279
6	636	619
8	540	523
12	401	402
H 2 4		
-12	253	247
-4	305	342
H 2 5		
-14	445	436
-8	753	706
-6	292	331
-2	554*	678
0	218	239
2	674	724
6	321	309
8	426	418
H 2 6		
-12	546*	476
-6	283	238
-4	210	195
-2	440*	368
2	528*	455
H 3 0		
-14	193	211
-8	618	606
-4	1022	987
-2	1841*	1734
0	151	144
2	1396	1394
4	691	682
6	727	725
8	628	650
12	576	576
H 3 1		
-12	272	278
-10	267	271
-8	390	347
-6	506	498
-4	140	115
-2	224*	258
0	445	426
2	553	558
4	151	131
6	287	292
8	342	333
12	217	194
H 3 2		
-12	578	576
-10	220	219
-8	846	851
-6	226	228
-4	407	415
-2	1430*	1519
0	218	252
2	782	807
4	283	279
6	636	619
8	540	523
12	401	402
H 3 3		
-15	385	406
-11	636	623
-9	998	1004
-5	1088	1112
-3	658	653
-1	1467*	1532
1	852	896
3	237	228
5	1141	1127
7	421	427
9	629	642
H 3 4		
9	192*	108
H 3 5		
-13	266*	47
-11	318	280
-9	793	805
-7	334	347
-5	638*	730
-3	200	157
-1	894*	974
1	641	668
3	206	227
5	677	649
7	233	242
9	538	509
H 3 7		
-14	214	189
H 4 0		
2	166	172
4	529	549
8	164	192
10	424	405
H 4 1		
-12	418	437
-10	212	183
-8	153	153
-4	201	206
-2	521	518
0	544	541
2	643	656
8	301	284
12	222	234
H 4 2		
-14	214	189
H 4 3		
-14	108*	21
-10	217	251
-6	182	182
-2	214	206
0	661	671
2	377	369
4	173	147
H 4 4		
-10	345	344
-4	191	249
10	209	206
2	186	169
4	234	262
H 4 5		
-12	256	259
-8	279	316
-2	228	252
2	299	348
8	248*	183
H 4 6		
-8	261	280
-2	259*	178
H 4 7		
-11	331	361
-7	258	258
-5	799	779
-3	235	246
-1	328	314
1	208	239
3	171	122
5	680	707
9	254	271
H 4 8		
-14	235	210
-8	458	462
-4	175	163
0	415	427
4	257	248

H	OBS	CALC
H 4 9		
-13	442	425
-11	344	348
-9	296	300
-7	1101	1118
-5	351	331
-3	1159	1132
-1	447	427
1	897	878
3	1284	1319
7	708	697
9	343	361
11	514	499
H 5 3		
-9	181	211
-7	265	287
-5	239	282
-3	405	378
-1	252	299
3	176	167
7	272*	205
H 5 4		
1	566	548
3	808	773
5	203	208
7	595	588
9	191*	130
H 5 5		
-7	301*	236
1	183	195
H 5 6		
-11	352	376
-9	222	216
-7	390	402
-3	741	783
-1	234	202
1	279	232
3	532	500
5	220	220
H 6 0		
0	1694	1726
2	288	291
4	561	563
6	505	517
8	429	463
10	707	719
H 6 1		
-14	180*	21
-4	216	175
-2	177*	245
0	184	183
H 6 2		
-14	574	573
-10	442	427
-8	309	308
-6	974	993
-4	494*	593
-2	175	200
0	1405	1419
2	469	493
4	602	607
6	289	299
8	301	303
10	630	621
H 6 3		
-6	188*	58
2	171	166
H 6 4		
-10	571	544
-6	667*	606
-4	843	828
0	621	590
2	276	251
4	748	748
6	211	202
H 6 6		
-10	512	482
-6	363	354
-4	473	455
0	485	476
4	466	422
H 7 0		
3	141	133
5	354	376
7	305	326
H 7 1		
-13	185	143
-11	211	169
-9	214	214
-5	744	752
-3	134	103
-1	300	294
1	512	547
5	402	401
9	387	376

H	OBS	CALC
H 7 2		
-7	260	275
-5	339	317
-3	263	250
-1	169	176
3	259	274
5	315	317
7	176	130
H 7 3		
-9	343	362
-5	454	444
-1	432	441
1	191	187
5	478	465
9	235	208
H 7 4		
-9	231*	164
-7	266	285
-1	174	158
5	237	192
H 7 5		
-11	278*	200
-5	473	456
-1	235	224
1	251	263
H 7 6		
-3	232	233
3	208*	101
H 7 7		
-5	248	220
-1	223	191
H 8 0		
4	151*	75
6	177	134
8	199	188
H 8 1		
-12	573	579
-10	197	193
-8	611	600
-6	339	315
-4	526	532
-2	1276	1288
2	723	752
4	532	576
6	666	657
8	409	413
12	601	604
H 8 2		
2	254	253
H 8 3		
-8	607	583
-6	209	309
-4	422	377
-2	940	902
0	266	223
2	764	763
4	162	165
6	479	474
8	546	558
H 8 4		
-14	207	218
-10	542	556
-6	331	308
-2	207	153
0	242	220
2	582	523
4	193	155
6	366	333
H 8 5		
-8	726	682
-6	202	214
-4	215	156
-2	700	661
0	242	220
2	582	523
4	193	155
6	366	333
H 8 6		
-4	257	214
-2	275	248
H 8 7		
-6	257	214
-2	275	248
H 8 8		
3	188	194
7	185	143
H 9 0		
-11	331	361
-9	281	281
-7	258	258
-5	799	779
-3	235	246
-1	328	314
1	208	239
3	171	122
5	680	707
9	254	271
H 9 1		
-7	185	173
-3	166	160

H	OBS	CALC
H 9 2		
-9	328	313
-5	399	389
-1	362	365
1	361	341
5	242	201
H 9 3		
-11	197	218
-9	542	556
-5	331	308
-3	207	153
-1	657	652
3	169	112
5	604	603
9	188	199
H 9 4		
-7	211*	133
-3	182	171
H 9 5		
-9	328	313
-5	399	389
-1	362	365
1	361	341
5	242	201
H 10 0		
0	608	615
4	424	439
6	259	253
10	395	404
H 10 1		
-2	246	239
0	244	290
H 10 2		
-10	389	400
-6	292	279
-4	366	369
0	555	568
4	406	411
6	203	213
H 10 3		
0	223	221
2	184	159
H 10 4		
-10	386*	323
-6	307	302
-4	353	322
0	431	419
4	349	331
6	193	166
H 10 5		
-4	183*	107
-2	199	164
H 10 6		
-4	243	223
H 11 0		
1	440	428
3	466	482
7	600	645
9	213	238
H 11 1		
-3	195	201
H 11 2		
-7	662	655
-3	486	458
-1	168	164
1	387	426
3	591	606
7	390	407
H 11 4		
-8	175	123
-6	166	144
-2	177	181
2	296	291
8	198	191
H 12 2		
-6	352	300
-2	175	211
0	457	445
H 12 3		
-8	268	210
-2	300	254
H 12 4		
-6	232	236
-4	305	279
0	248*	187

H	OBS	CALC
H 13 1		
-5	409	404
-1	302	352
1	194*	256
5	426	453
H 13 3		
-5	429	424
-1	276	278
1	234	277
H 14 0		
0	214	179
H 14 1		
-4	238	235
-2	408	427
2	346	338

F580W020

H	OBS	CALC
H 0 0		
0	0	5024
2	854	786
4	544	619
6	1415	1391
8	1015	1029
10	939	932
12	53	71
14	687	699
H 0 2		
-14	735	759
-12	138	132
-10	1032	1039
-8	607	621
-6	1534	1510
-4	1701	1632
-2	132	181
0	1794	1938
2	1455	1432
4	1463	1420
6	431	417
8	537	513
10	1150	1091
12	162	159
H 0 4		
-14	825	859
-12	383	394
-10	742	730
-8	261	258
-6	1382	1334
-4	1280	1211
-2	219	247
0	1147	1305
2	530	537
4	1029	974
6	575	539
8	327	288
10	590	548
H 0 6		
-12	323	318
-10	1002	987
-8	90	68
-6	523	486
-4	961	939
-2	425	453
0	538	582
2	215	208
4	801	724
6	392	344
H 0 8		
-8	279	247
-6	434	379
-4	346	319
-2	307	313
0	559	545
H 1 0		
1	490	434
3	1282	1243
5	283	272
7	715	704
9	243	252
11	308	298
13	119	123
15	81	22
H 1 1		
-15	36	92
-13	110	106
-11	157	165
-9	26	28
-7	312	315
-5	175	142
-3	820	767
-1	19	48
1	21	17
3	561	582
5	100	92
7	340	353
9	29	32
11	136	134
13	104	101
H 1 2		
-15	76	78
-13	437	458
-11	64	68
-9	27	41
-7	1268	1242
-5	52	34
-3	306	335
-1	433	458
1	815	886
3	594	621
5	236	233
7	745	713
9	68	51
11	221	212
13	228	223
H 1 3		
-15	34	47
-13	33	68
-11	29	37
-9	68	72
-7	383	379
-5	361	337
-3	491	490
-1	182	192
1	27	48
3	264	292
5	30	34
7	290	276
9	34	43
11	154	134
H 1 4		
-15	34	27
-13	334	339
-11	295	301
-9	20	49
-7	537	520
-5	96	90
-3	896	911
-1	116	129
1	156	158
3	718	758
5	32	33
7	265	241
9	35	44
11	290	262
H 1 5		
-13	141	132
-11	32	22
-9	31	45
-7	327	325
-5	144	132
-3	230	241
-1	31	5
1	112	115
3	210	196
5	36	40
7	207	190
9	37	13
H 1 6		
-13	423	434
-11	150	162
-9	33	18
-7	513	482
-5	33	42
-3	441	449
-1	110	121
1	140	145
3	231	218
5	30	56
7	345	296
H 1 7		
-11	36	14
-9	36	38
-7	164	165
-5	82	84
-3	188	191
-1	37	5
1	40	41
3	133	102
H 1 8		
-7	167	168
-5	39	56
-3	377	377
-1	40	54
H 2 0		
0	256	202
2	787	789
4	278	282
6	71	85
8	320	329
10	81	75
12	206	207
14	34	30
H 2 1		
-14	84	77
-12	835	826
-10	150	149
-8	647	624
-6	604	597
-4	1073	1005
-2	1768	1663
0	150	138
2	1276	1349
4	670	690
6	710	731
8	645	650
10	31	28
12	610	594
14	192	185
H 2 2		
-14	130	136
-12	314	314
-10	277	273
-8	402	394
-6	558	543
-4	151	116
-2	220	267
0	410	446
2	516	573
4	144	120
6	269	287
8	338	334
10	78	87
12	202	198
H 2 3		
-14	34	43
-12	622	644
-10	220	235
-8	916	907
-6	260	259
-4	427	429
-2	1466	1513
0	220	260
2	710	784
4	274	282
6	462	611
8	135	116
10	38	19
12	103	102
14	136	136
H 3 0		
1	86	76
3	373	369
5	115	156
7	157	161
9	171	165
11	110	102
13	33	51
H 3 1		
-15	442	471
-13	322	333
-11	717	713
-9	1000	986
-7	26	51
-5	1089	1026
-3	1634	1517
-1	1607	1547
1	463	524
3	717	769
5	1920	2002
7	222	242
9	564	576
11	491	499
13	450	451
H 3 2		
-15	74	60
-13	114	105
-11	29	52
-9	27	7
-7	212	201
-5	169	146
-3	265	241
-1	304	301
1	262	276
3	138	144
5	125	117
7	134	129
9	30	26
11	33	24
13	112	92
H 3 3		
-15	456	482
-13	151	156
-11	688	706
-9	1095	1089
-7	140	140
-5	1157	1166
-3	690	707
-1	1432	1517
1	793	885
3	212	222
5	1083	1114
7	409	421
9	623	607
11	194	191
H 3 4		
-15	34	25
-13	32	72
-11	112	109
-9	130	119
-7	141	144
-5	139	124
-3	174	186
-1	28	4
1	29	37
3	138	151
5	110	94
7	34	59
9	96	90
H 3 5		
-13	95	82
-11	322	324
-9	925	919
-7	409	401
-5	766	763
-3	171	175
-1	917	1001
1	634	674
3	189	197
5	645	618
7	254	237
9	476	474
H 3 6		
-13	36	64
-11	34	31
-9	33	1
-7	114	94
-5	80	55
-3	77	82
-1	124	125
1	85	81
3	38	41
5	38	45
7	39	66
H 3 7		
-11	279	267
-9	398	386
-7	340	330
-5	750	733
-3	39	45
-1	414	430
1	478	480
3	268	258
H 3 8		
-7	38	51
-5	38	44
-3	38	50
-1	39	6
H 4 0		
0	66	87
2	183	177
4	540	538
6	87	94
8	180	186
10	402	399
12	134	155
14	79	55
H 4 1		
-14	119	116
-12	442	457
-10	189	184
-8	177	166
-6	119	118
-4	205	197
-2	541	517
0	546	548
2	644	672
4	62	43
6	83	99
8	277	290
10	210	213
12	231	251
H 4 2		
-14	211	211
-12	180	173
-10	251	250
-8	27	39
-6	183	172
-4	53	46
-2	222	204
0	627	657
2	340	360
4	145	134
6	126	126
8	31	63
10	138	124
12	103	83
H 4 3		
-14	113	103
-12	275	284
-10	103	104
-8	431	442
-6	144	147
-4	83	79
-2	723	764
0	260	292
2	212	232
4	77	45
6	185	199
8	145	145
10	166	163
H 4 4		
-14	131	127
-12	195	205
-10	367	377
-8	106	93
-6	28	37
-4	217	216
-2	109	103
0	207	213
2	161	171
4	239	255
6	33	53
8	99	92
10	186	157
H 4 5		
-14	111	88
-12	282	313
-10	161	151
-8	308	312
-6	30	51
-4	31	48
-2	249	266
0	114	95
2	306	335
4	172	172
6	35	43
8	191	190
H 4 6		
-12	89	73
-10	124	114
-8	34	56
-6	205	208
-4	33	24
-2	118	118
0	251	254
2	136	145
4	38	70
6	38	43
H 4 7		
-10	113	120
-8	304	303
-6	36	10
-4	35	34
-2	185	184
0	91	86
2	183	182
H 4 8		
-6	38	37
-4	87	95
-2	37	6
H 5 0		
1	1323	1228
3	986	985
5	87	73
7	1246	1291
9	382	396
11	357	360
13	395	403
H 5 1		
-13	146	128
-11	208	215
-9	28	14
-7	179	161
-5	163	136
-3	408	473
-1	81	30
1	171	156
3	429	442
5	66	44
7	288	254
9	31	77
11	80	76
13	94	99
H 5 2		
-13	474	473
-11	395	390
-9	382	338
-7	1163	1174
-5	382	357
-3	1160	1150
-1	443	454
1	849	889
3	1238	1306
5	92	88
7	676	687
9	362	363
11	513	506
H 5 3		
-13	33	22
-11	32	27
-9	209	221
-7	268	266
-5	255	264
-3	402	408
-1	304	311
1	28	42
3	170	180
5	139	129
7	186	188
9	72	30
11	188	123
H 5 4		
-13	676	684
-11	364	360
-9	126	118
-7	976	975
-5	371	364
-3	874	888
-1	303	314
1	516	555
3	758	776
5	191	200
7	568	552
9	125	129
H 5 5		
-13	131	135
-11	33	40
-9	32	20
-7	254	259
-5	34	31
-3	114	121
-1	31	44
1	160	168
3	156	152
5	37	43
7	179	164
H 5 6		
-11	447	445
-9	272	263
-7	489	460
-5	169	154
-3	801	815
-1	221	218
1	221	223
3	498	486
5	242	223
H 5 7		
-9	86	48
-7	147	151
-5	36	48
-3	148	150
-1	80	69
1	37	17
3	92	91
H 6 0		
0	1759	1703
2	310	297
4	599	588
6	529	548
8	443	463
10	722	747
12	118	99
H 6 1		
-14	34	26
-12	32	34
-10	89	77
-8	135	138
-6	136	123
-4	216	197
-2	224	221
0	198	175
2	90	83
4	67	23
6	28	29
8	100	91
10	80	73
12	85	99
H 6 2		
-14	613	640
-12	32	30
-10	480	481
-8	344	335
-6	1055	1026
-4	661	624
-2	189	193
0	1402	1428
2	487	506
4	582	594
6	297	303
8	305	309
10	617	627
12	35	50
H 6 3		
-14	85	62
-12	132	143
-10	127	113
-8	73	63
-6	67	52
-4	27	19
-2	94	99
0	152	146
2	150	159
4	146	143
6	32	54
8	33	42
10	87	64
H 6 4		
-12	170	180
-10	618	618
-8	68	40
-6	653	653
-4	873	873
-2	29	55
0	569	605
2	254	262
4	717	730
6	197	198
8	109	79
H 6 5		
-12	34	10
-10	33	32
-8	100	111
-6	147	127
-4	74	63
-2	105	129
0	112	105
2	33	46
4	36	31
6	37	27
H 6 6		
-10	575	569
-8	34	30
-6	386	384
-4	515	510
-2	189	185
0	454	467
2	35	39
4	422	412
H 6 7		
-8	35	5
-6	36	17
-4	35	6
-2	110	49
0	36	26
2	38	60
H 7 0		
1	25	3
3	166	160
5	374	374
7	340	355
9	124	125
11	33	27
13	35	76
H 7 1		
-13	151	156
-11	196	195
-9	248	236
-7	117	36
-5	804	775
-3	101	80
-1	317	303
1	546	560
3	85	63
5	395	411
7	127	27
9	370	382
11	33	28
H 7 2		
-13	75	75
-11	31	4
-9	111	104
-7	285	288
-5	342	323
-3	274	277
-1	163	154
1	27	53
3	255	283
5	309	311
7	153	156
9	93	72
11	35	59
H 7 3		
-13	35	67
-11	153	149
-9	400	385
-7	30	32
-5	490	472
-3	25	58
-1	439	455
1	168	189
3	30	22
5	454	469
7	34	31
9	209	207
H 7 4		
-13	174	185
-11	33	27
-9	183	172
-7	296	307
-5	204	195
-3	142	156
-1	143	139
1	29	9
3	147	161
5	213	201
7	121	128
9	92	98
H 7 5		
-11	257	265
-9	207	201
-7	32	41
-5	493	498
-3	31	46
-1	214	228
1	234	249
3	35	59
5	179	170
7	37	24
H 7 6		
-9	81	66
-7	39	114
-5	161	155
-3	210	231
-1	104	105
1	103	85
3	114	115

H	OBS	CALC
H 7 7		
-7	39	31
-5	221	211
-3	35	24
-1	227	220
H 8 0		
0	164	155
2	199	186
4	114	80
6	115	115
8	197	201
10	85	63
12	86	67
H 8 1		
-12	635	638
-10	219	206
-8	673	637
-6	368	351
-4	589	559
-2	1379	1315
0	26	39
2	783	761
4	593	596
6	670	685
8	427	424
10	35	53
12	605	630
H 8 2		
-12	132	115
-10	32	61
-8	136	121
-6	151	130
-4	81	51
-2	129	99
0	27	7
2	246	239
4	32	32
6	32	5
8	125	127
10	34	28
H 8 3		
-12	667	669
-10	246	248
-8	657	628
-6	359	345
-4	416	415
-2	933	934
0	239	243
2	750	769
4	172	166
6	473	480
8	574	559

H	OBS	CALC
H 8 4		
-12	174	183
-10	73	52
-8	32	35
-6	104	117
-4	94	83
-2	86	74
0	30	22
2	156	166
4	34	28
6	35	18
8	91	93
H 8 5		
-10	136	143
-8	757	766
-6	163	255
-4	186	169
-2	672	687
0	234	242
2	516	522
4	160	144
6	334	323
H 8 6		
-8	92	60
-6	34	17
-4	73	61
-2	134	133
0	34	42
2	35	67
H 8 7		
-4	257	245
-2	273	263
H 9 0		
1	27	23
3	182	188
5	60	34
7	157	158
9	80	25
11	90	76
H 9 1		
-11	398	394
-9	327	317
-7	266	256
-5	866	820
-3	277	255
-1	357	331
1	295	274
3	140	137
5	733	725
7	90	45
9	260	291
11	115	138

H	OBS	CALC
H 9 2		
-11	34	82
-9	88	8
-7	179	169
-5	71	54
-3	171	173
-1	28	38
1	29	70
3	75	105
5	73	53
7	175	158
9	37	14
H 9 3		
-11	282	237
-9	621	615
-7	115	103
-5	356	343
-3	171	170
-1	661	672
1	159	154
3	106	111
5	629	624
7	95	79
9	186	193
H 9 4		
-11	34	45
-9	34	46
-7	163	161
-5	78	63
-3	140	147
-1	30	15
1	32	58
3	86	87
5	34	22
7	36	78
H 9 5		
-9	362	366
-7	113	87
-5	422	429
-3	119	111
-1	381	379
1	352	357
3	34	19
5	209	208
H 9 6		
-7	106	118
-5	34	21
-3	102	97
-1	34	32
1	35	64
H 10 0		
0	640	641
2	117	107

H	OBS	CALC
H 10 0		
4	478	466
6	274	266
8	138	145
10	439	435
H 10 1		
-10	143	153
-8	155	165
-6	112	102
-4	151	146
-2	279	276
0	293	284
2	114	87
4	31	48
6	33	15
8	33	9
10	149	154
H 10 2		
-10	440	440
-8	174	168
-6	330	314
-4	403	397
-2	110	120
0	586	596
2	30	68
4	435	434
6	209	225
8	112	111
H 10 3		
-10	166	155
-8	33	31
-6	31	14
-4	30	30
-2	100	96
0	224	230
2	180	189
4	127	128
6	34	41
8	110	105
H 10 4		
-10	389	385
-8	118	106
-6	329	330
-4	343	338
-2	87	84
0	428	441
2	33	74
4	343	341
6	173	157
H 10 5		
-8	166	171
-6	33	112
-4	99	113

H	OBS	CALC
H 10 5		
-2	195	193
0	139	133
2	34	28
H 10 6		
-4	237	227
-2	139	124
H 11 0		
1	460	460
3	529	513
5	73	60
7	550	680
9	236	252
H 11 1		
-9	119	122
-7	84	40
-5	32	48
-3	244	211
-1	142	115
1	96	80
3	135	112
5	159	148
7	81	32
9	35	31
H 11 2		
-9	130	133
-7	732	711
-5	189	137
-3	495	499
-1	178	183
1	436	449
3	636	643
5	33	44
7	405	413
H 11 3		
-9	82	57
-7	104	59
-5	32	35
-3	115	99
-1	96	60
1	78	53
3	88	81
5	34	7
H 11 4		
-9	35	64
-7	513	522
-5	161	172
-3	541	545
-1	130	115
1	224	239
3	491	491

H	OBS	CALC
H 11 5		
-7	142	132
-5	85	65
-3	75	61
-1	134	131
1	35	5
H 12 0		
0	607	587
2	31	66
4	143	129
6	183	158
8	145	125
H 12 1		
-8	175	148
-6	188	177
-4	114	119
-2	214	190
0	30	36
2	352	332
4	33	45
6	98	93
H 12 2		
-8	73	53
-6	353	334
-4	195	170
-2	196	201
0	510	490
2	86	56
4	184	173
6	80	48
H 12 3		
-8	242	229
-6	110	91
-4	94	91
-2	275	267
0	32	19
2	185	173
4	95	94
H 12 4		
-6	273	255
-4	324	320
-2	114	130
0	238	216
2	85	56
H 13 0		
1	80	53
3	93	61
5	154	143

H	OBS	CALC
H 13 1		
-7	34	85
-5	434	447
-3	114	138
-1	370	391
1	241	284
3	33	98
5	470	489
H 13 2		
-7	83	59
-5	143	152
-3	117	106
-1	33	70
1	34	64
3	102	85
H 13 3		
-5	448	479
-3	34	98
-1	287	307
1	271	301
H 14 0		
0	208	180
2	125	76
4	34	20
H 14 1		
-4	249	267
-2	451	468
0	113	96
2	368	372
H 14 2		
-2	95	47
0	123	84

H	OBS	CALC
H 0 0		
-14	641	655
-10	949	955
-8	1005	1001
-6	1474	1466
-4	539*	608
-2	1002*	849
0	0	5048
2	996*	849
4	537*	608
6	1457	1466
8	984	1001
10	938	955
14	635	655
H 0 2		
-14	675	679
-13	124	130
-12	209*	131
-10	967	1019
-8	625	623
-7	225	284
-6	1513	1510
-5	87	120
-4	1697	1694
-3	46	92
-2	224	218
-1	53	87
0	2220*	2112
1	184	172
2	1635*	1517
3	73	77
4	1528*	1460
6	549	537
8	452	455
10	1168	1179
12	161	208
H 0 4		
-14	730	738
-13	124	125
-12	364	383
-11	125	142
-10	691	701
-9	73*	168
-8	261	247
-7	187	217
-6	1320	1293
-5	107	117
-4	1395*	1331
-3	309	299
-2	171	207
-1	91	41
0	1413*	1346
2	686	657
3	222	218
4	1033	996
5	84*	12
6	674	654
8	259	279
10	649	651

H	OBS	CALC
H 1 1		
3	621	600
5	70	50
7	384	389
10	62	33
11	100	95
13	156	165
H 1 2		
-15	91	45
-13	428	462
-12	54	3
-10	66	96
-9	132*	33
-7	1224	1218
-5	56	30
-4	90	97
-3	307	338
-1	447	482
1	928	911
3	715	710
4	64	58
7	748	740
9	137	121
11	93	147
13	260	280
H 1 3		
-15	60	56
-14	73	59
-13	67	71
-11	52	44
-10	90	76
-9	76	82
-7	396	378
-6	62	72
-5	328	316
-4	83	77
-3	476	466
-1	233	267
0	56	66
1	62	61
3	332	323
5	61	46
7	325	322
11	90	98
H 1 4		
-14	92	89
-13	314	302
-11	274	276
-9	62	70
-7	573	584
-6	133	129
-5	82	76
-4	82	76
-3	880	898
-2	51	68
-1	54	23
0	138	138
1	130	101

H	OBS	CALC
H 2 0		
0	173	158
2	908	873
4	337	339
5	48	64
6	80	82
8	373	386
10	109	117
12	213	207
H 2 1		
-15	75	68
-14	82	87
-13	107*	42
-12	758	746
-10	105	118
-9	126*	38
-8	612	619
-7	102	76
-6	520	528
-5	90	80
-4	995	969
-2	1788*	1700
-1	50	49
0	203	190
1	40	23
2	1385	1330
4	737	712
6	645	636
7	123*	48
8	678	677
10	59	31
11	145*	46
12	576	564
14	197	192
H 2 2		
-14	134	148
-12	293	307
-11	69	98
-10	231	243
-9	91	115
-8	410	404
-6	583	577
-5	89	97
-4	79	47
-3	98	96
-2	258	289
0	420	443
2	675	677
3	53	22
4	61	37
6	253	256
8	398	395
12	224	231
H 2 3		
-14	67	53
-12	555	565
-11	87	107
-10	211	199

H	OBS	CALC
H 2 6		
-9	126	143
-8	211	193
-6	136	128
-5	64	54
-3	78	88
-2	233	256
0	102	88
2	206	225
5	74	60
6	155	142
H 2 7		
-12	307	325
-9	106	116
-8	516	483
-7	62	23
-6	328	298
-5	135	148
-4	138	144
-2	399	425
-1	67	51
0	94	110
1	104	86
2	476	458
4	167	153
H 2 8		
-8	140	128
-6	75*	11
-5	76	88
-4	81	56
-2	165	175
0	70	13
H 3 0		
-13	62	84
-11	101	85
-9	121	121
-7	174	185
-5	92	84
-3	303	293
-1	138	143
1	142	143
3	305	293
5	94	84
7	190	185
9	130	121
11	94	85
13	69	54
H 3 1		
-15	425	472
-14	103	135
-13	301	309
-12	144	115
-11	732	782
-10	96	66
-9	920	956
-8	77	117

H	OBS	CALC
H 3 4		
-13	94	81
-11	83	59
-9	102	88
-7	151	147
-6	58	63
-5	89	45
-3	132	149
1	71	87
3	103	95
4	56	41
5	112	96
7	86	77
H 3 5		
-13	93	104
-12	140	189
-11	290	294
-10	70	118
-9	418	890
-8	207	198
-7	425	410
-6	157	142
-5	781	784
-4	67	72
-3	102	227
-2	127*	201
-1	875*	1006
1	765*	836
2	151	150
3	171	183
4	77	20
5	721	714
7	310	317
8	97	77
9	517	524
H 3 6		
-9	60	30
-7	62	44
-5	64	46
-3	95	89
-1	93	63
1	81	76
H 3 7		
-11	248	241
-10	66	43
-9	434	395
-8	203	197
-7	326	312
-6	161	172
-5	703	762
-3	76	100
-2	115	135
-1	379	418
1	576	612
2	148	171
3	283	286
4	86	34

H	OBS	CALC
H 4 3		
-8	431	445
-7	86	67
-6	89	91
-5	66	74
-4	80	70
-2	727*	829
0	249	265
2	231	250
6	172	179
8	204	208
10	191	181
H 4 4		
-14	89	89
-12	210	210
-11	70	44
-10	305	310
-9	87	78
-8	103	72
-5	66	54
-4	158	149
-2	148	153
0	193	206
2	201	210
4	151	157
6	66	37
8	170	157
10	181	154
H 4 5		
-14	78	64
-12	290	298
-10	131	115
-9	77	65
-8	305	297
-6	104	98
-2	303	340
0	102	86
2	318	348
4	125	114
7	66	29
8	281	266
H 4 6		
-12	76	58
-10	119	92
-8	97	77
-6	170	164
-4	88	66
-2	169	197
0	206	213
2	99	115
4	65	22
H 4 7		
-10	117	94
-8	297	291
-6	84	66
-2	205	235

H	OBS	CALC
H 5 2		
11	454	450
12	62	44
H 5 3		
-13	73	65
-11	80	75
-10	80	95
-9	238	244
-7	331	342
-6	49	35
-5	192	184
-4	99	93
-3	440	464
-1	381	416
3	248	267
5	167	162
7	279	284
8	64	29
10	61	36
11	129	137
H 5 4		
-14	92	94
-13	584	586
-11	339	340
-10	138	126
-9	88	83
-8	54	69
-7	907	891
-6	92	95
-5	361	367
-4	151	162
-3	768*	833
-1	290	310
0	67	68
1	460	497
3	825	853
4	96	114
5	168	151
7	565	553
9	192	192
H 5 5		
-13	148	146
-11	92	80
-10	75	50
-8	72	76
-7	312	301
-6	71	74
-5	73	87
-3	149	172
-1	89	99
0	73	108
1	197	217
3	240	256
6	69	29
7	217	210
H 5 6		

H	OBS	CALC
10	649	651
H 0 6		
-12	248	264
-10	819*	905
-8	128	132
-7	206	227
-6	456	428
-5	134	117
-4	1058*	986
-3	1184	215
-2	501	476
-1	130	101
0	697	660
1	81	56
2	244	232
3	132	114
4	776	768
5	74	38
6	510	509
7	108	105
H 0 8		
-8	274	265
-7	150	167
-6	382	340
-4	337*	406
-3	181	206
-2	325	311
-1	146	142
0	667	611
H 1 0		
-13	162	170
-11	263	261
-9	278	283
-7	700	697
-5	258	245
-3	1373	1322
3	1387*	1322
5	258	245
7	703	697
9	279	283
11	250	261
13	161	170
H 1 1		
-15	72	99
-14	85	77
-13	153	151
-12	52	48
-11	147	159
-10	55	29
-8	72	80
-7	302	312
-6	54	104
-5	118	102
-4	59	29
-3	854	794
-1	104	98

H	OBS	CALC
0	138	138
1	130	101
2	58	18
3	858	840
7	258	256
9	95	87
11	252	255
H 1 5		
-13	115	109
-7	348	327
-6	72	73
-5	122	107
-4	72	46
-3	196	213
0	90	103
1	133	112
3	280	268
5	86	64
7	194	204
H 1 6		
-13	331	369
-11	166	193
-7	514	482
-4	112	111
-3	382*	455
-1	153	153
0	60	70
1	132	117
3	343	335
4	98	81
6	72	30
7	336	317
H 1 7		
-8	188	176
-7	74	61
-6	178	164
-5	70	69
-3	167	182
3	180	162
H 1 8		
-9	150	138
-7	224	207
-6	78	68
-3	362	382
-1	117	135
0	88	113
H 2 0		
-14	62	29
-12	210	207
-10	109	117
-8	374	386
-6	81	82
-5	53	64
-4	327	339
-2	870	873

H	OBS	CALC
-11	87	107
-10	211	199
-9	115	87
-8	857	850
-6	151	135
-5	1656	1701
-4	108	130
-3	1576	1603
-2	119	125
-1	1609	1661
0	40	62
-2	1366*	1543
-1	54	101
1	580	638
3	779	783
4	65	43
5	2115	2147
7	319	319
8	147	117
9	550	561
10	145*	79
13	431	429
14	97	95
H 3 2		
-13	80	80
-11	66	64
-7	160	158
-6	49	40
-5	129	111
-3	302	297
-1	190	183
1	251	248
3	164	172
5	75	40
7	99	106
13	90	70
H 3 3		
-15	431	450
-13	157	154
-12	137	179
-11	672	679
-9	1065	1058
-8	182	188
-7	171	176
-6	108	143
-5	1178	1186
-4	63	78
-3	738	775
-2	167*	252
-1	1347*	1564
0	76	79
1	915*	1032
2	73	52
3	208	209
5	1218	1218
6	68	63
7	504	506
8	72	25
9	620	626
11	275	283

H	OBS	CALC
4	86	34
H 4 0		
-12	157	149
-10	329	333
-8	264	266
-6	96	101
-5	59	42
-4	434	440
-2	234	254
2	248	254
4	440	440
5	68	42
6	104	101
8	256	266
10	328	333
12	153	149
14	61	21
H 4 1		
-14	98	85
-12	421	431
-10	173	165
-8	210	221
-6	120	128
-4	215	232
-3	48	30
-2	554	588
0	505	514
2	688	711
3	45	62
6	69	78
7	61	25
8	337	347
10	211	200
11	89*	25
12	269	265
H 4 2		
-15	65	39
-14	166	139
-12	169	146
-11	52	39
-10	194	205
-8	100	109
-6	126	117
-5	57	38
-2	287	288
-1	57	57
0	550	580
2	382	389
6	135	129
8	110	107
10	101	75
12	132	133
H 4 3		
-14	84	64
-12	270	272
-10	98	87

H	OBS	CALC
-6	84	66
-2	205	235
0	85	61
2	178	202
H 4 8		
-4	100	102
H 5 0		
-13	370	419
-11	278	288
-9	386	389
-7	1185	1224
-5	90	47
-3	834*	909
-1	1116	1174
1	1139	1174
3	867	909
7	1221	1224
9	402	389
11	284	288
13	399	419
H 5 1		
-13	175	186
-11	230	248
-8	73	73
-7	251	253
-5	206	207
-3	561	587
-1	108	109
0	64	66
1	238	247
3	525	545
5	51	45
7	348	354
9	145	126
10	77	36
11	101	97
12	69	10
13	166	173
H 5 2		
-14	92	56
-13	436	436
-11	326	323
-10	83	91
-9	291	318
-7	1110	1103
-6	107	92
-5	331	385
-4	51	42
-3	1050	1077
-1	454	473
0	123	146
1	777	801
3	1280	1306
5	73	69
7	668	657
9	394	378

H	OBS	CALC
H 5 6		
-11	403	385
-10	134	105
-9	222	224
-7	471	462
-6	100	111
-5	138	128
-4	112	137
-3	705*	765
-2	63	19
-1	268	287
0	106	127
1	161	166
2	62	27
3	530	540
4	83	63
5	247	237
6	91	75
H 5 7		
-7	174	183
-4	72	92
-3	171	179
-1	96	115
H 6 0		
-12	72	53
-10	753	796
-8	456	481
-7	53	29
-6	610	644
-4	616	641
-2	368	395
0	1696*	1842
2	388	395
4	634	641
6	632	644
7	70	29
8	480	481
9	58	78
10	790	796
H 6 1		
-8	135	155
-6	82	75
-4	157	145
-2	205	212
0	107	90
2	50	45
8	71	51
10	63	41
12	94	97
H 6 2		
-14	583	585
-13	79	60
-12	94	72
-11	73	99
-10	496	513

FS&SWo 15 (cont.)

H	OBS	CALC
	H 6 2	
-8	361	349
-7	123	118
-6	1044	1063
-5	70	66
-4	725	731
-3	93	99
-2	134	136
0	1443*	1510
1	63	48
2	616	639
3	98	98
4	629	637
6	403	409
8	326	324
10	729	716
12	105	91
	H 6 3	
-12	129	134
-10	91	77
-6	89	83
-3	58	74
-2	74	70
0	122	107
2	156	167
4	81	83
6	68	52
10	71	44
	H 6 4	
-13	146	128
-12	191	178
-11	69	84
-10	595	603
-8	73	65
-7	193	194
-6	641	648
-5	87	76
-4	916	935
-3	123	120
-2	95	109
-1	66	53
0	626*	693
2	302	332
3	103	111
4	755	780
6	351	344
7	75	38
8	70	65
	H 6 5	
-8	97	110
-6	95	81
-2	126	105
0	69	65
	H 6 6	
-11	133	122
-10	559	558

H	OBS	CALC
	H 7 1	
-13	71	64
-11	140	140
-10	72*	8
-9	165	162
-7	80	77
-5	605	627
-3	154	154
-1	178	188
1	428	449
5	317	314
7	70	49
9	295	294
	H 7 2	
-13	80	79
-9	98	95
-7	270	288
-5	332	342
-3	253	263
-1	121	118
1	104	87
3	275	294
5	332	329
7	165	164
9	60	59
	H 7 3	
-11	97	95
-9	298	286
-7	80	73
-5	377	381
-2	64	24
-1	298	320
0	67	37
1	126	141
3	62	66
5	415	415
7	90	84
9	127	119
	H 7 4	
-13	163	155
-9	180	176
-7	282	286
-5	183	178
-3	134	149
-1	128	139
3	207	224
5	267	256
7	120	118
9	74	55
	H 7 5	
-11	189	201
-9	173	161
-7	85	91
-5	397	409
-1	142	145

H	OBS	CALC
	H 8 0	
4	54	34
5	65	60
6	189	182
8	286	283
12	130	122
	H 8 1	
-13	115	71
-12	572	583
-11	57	53
-10	206	187
-9	72	37
-8	573	613
-6	323	327
-5	95	90
-4	551	556
-2	1245	1270
2	735	746
4	604	610
6	629	620
8	465	461
11	82*	15
	H 8 2	
-12	141	152
-8	214	212
-6	204	199
-4	143	127
-2	241	237
0	91	70
1	56	42
2	333	341
4	150	137
6	93	71
8	186	191
10	99	89
	H 8 3	
-12	564	577
-10	237	228
-9	122	88
-8	598	594
-6	342	328
-5	115	91
-4	371	379
-3	55	50
-2	934	949
-1	97	93
0	238	234
1	62	48
2	725	733
4	228	230
5	82	69
6	446	437
8	635	606
	H 8 4	
-3	241	213
-2	114	115

H	OBS	CALC
	H 8 6	
-10	76	71
-9	89	70
-8	138	126
-4	80	71
-3	73	36
-2	193	216
2	92	101
	H 8 7	
-5	105	120
-4	211	222
-2	284	309
	H 9 0	
-7	125	114
-5	53	18
-4	65	50
-3	151	161
3	143	161
7	112	114
	H 9 1	
-12	88	55
-11	401	414
-9	334	341
-7	170	182
-6	67	74
-5	839	837
-3	330	312
-2	63	58
-1	421	404
1	364	341
3	188	167
5	806	800
9	298	291
11	218	208
	H 9 2	
-11	82	76
-8	72	54
-7	130	114
-5	58	38
-3	139	149
1	56	44
3	80	88
5	72	48
7	147	133
8	59	20
	H 9 3	
-12	77	111
-11	269	249
-10	61	54
-9	608	588
-8	76	50
-5	413	398
-3	241	213
-2	114	115

H	OBS	CALC
	H 9 6	
-7	111	91
-3	91	87
	H 10 0	
-10	338	348
-8	73	62
-6	198	220
-4	335	359
0	499	522
4	340	359
6	189	220
8	68	62
10	344	348
	H 10 1	
-10	173	188
-8	122	126
-7	67	67
-6	135	129
-4	177	180
-2	217	216
0	336	337
2	80	72
4	106	91
6	73	57
8	68*	6
10	197	181
	H 10 2	
-10	333	353
-8	105	107
-6	229	236
-4	296	302
0	484	504
4	308	317
6	213	212
8	74	47
	H 10 3	
-10	176	174
-4	86	84
-2	103	96
0	287	289
1	70	50
2	126	135
4	130	129
6	96	88
8	94	78
	H 10 4	
-10	300	307
-6	243	249
-4	294	290
0	359	375
2	70	61
4	244	249
6	144	137

H	OBS	CALC
	H 11 1	
-9	156	129
-7	116	118
-3	293	262
-1	184	159
3	205	184
5	183	159
7	133	116
	H 11 2	
-10	75	67
-9	140	136
-7	680	666
-6	82	37
-5	166	159
-4	75	60
-3	493	482
-1	221	210
0	83	62
1	439	436
3	677	663
5	66	34
7	413	411
	H 11 3	
-9	101	88
-7	152	125
-5	99	59
-3	183	164
-1	144	119
1	132	100
3	162	143
5	95	41
6	77	33
	H 11 4	
-8	64	70
-7	520	497
-6	98	61
-5	180	180
-4	94	86
-3	528	517
-1	181	162
0	97	63
1	215	225
3	535	530
4	84	46
	H 11 5	
-7	189	173
-6	64	24
-3	132	97
-2	61	7
-1	184	156
1	81	62
	H 12 0	
-8	142	116
-6	204	187

H	OBS	CALC
	H 12 3	
-8	173	157
-6	79	82
-4	93	69
-2	219	189
2	154	132
4	95	80
	H 12 4	
-6	262	231
-4	385	339
-2	100	116
0	267	231
2	116	82
	H 13 0	
-7	87	64
-5	195	195
-1	117	111
1	102	111
5	197	195
7	71	64
	H 13 1	
-5	358	378
-3	84	98
-1	288	303
1	224	243
5	391	401
	H 13 2	
-5	189	201
-3	73	61
-2	90	53
-1	133	108
1	131	118
	H 13 3	
-5	382	382
-1	222	247
1	237	251
	H 14 0	
-4	77	46
-2	168	118
0	209	149
2	171	118
4	87	46
	H 14 1	
-4	273	258
-2	505	466
0	73	76
2	377	342
	H 14 2	
-2	125	92
0	145*	78

H	OBS	CALC
-11	133	122
-10	559	558
-9	74	71
-7	148	131
-6	349	361
-4	562	616
-3	147	195
-2	176	204
0	475	521
2	116	118
3	106	120
4	435	463
	H 7 0	
-13	92	105
-11	60	57
-9	116	120
-7	324	343
-5	367	382
-3	165	181
-2	69	72
2	63	72
3	167	181
5	379	382
7	333	343
9	123	120
11	78	57
13	99	105

H	OBS	CALC
-5	397	409
-1	142	145
1	190	210
5	160	164
	H 7 6	
1	132	130
3	142	148
	H 7 7	
-5	164	163
-1	190	185
	H 8 0	
-12	108	122
-8	265	283
-6	172	182
-5	57	60
-2	300	304
-1	51	55
0	213	221
1	51	55
2	308	304

H	OBS	CALC
-12	211	217
-9	62	60
-8	82	88
-6	175	169
-5	63	83
-4	154	161
-3	69	62
-2	183	179
2	239	253
4	126	118
6	81	70
8	174	157
	H 8 5	
-10	143	124
-9	148	139
-8	698	689
-6	284	286
-5	140	113
-4	128	132
-2	656	701
-1	90	81
0	241	259
1	93	102
2	502	521
4	189	190
6	298	308

H	OBS	CALC
-3	241	213
-2	114	115
-1	687	686
1	284	272
3	97	98
5	690	683
7	161	154
9	205	215
	H 9 4	
-7	153	147
-3	101	104
0	57	30
3	73	69
7	76	62
	H 9 5	
-9	401	376
-8	134	115
-7	110	103
-6	87	84
-5	452	448
-2	114	112
-1	367	390
1	424	448
5	264	274

H	OBS	CALC
6	144	137
	H 10 5	
-8	127	123
-7	91	78
-6	120	109
-4	154	161
-2	176	173
0	158	160
	H 10 6	
-6	108	197
-4	197	198
-3	67	43
	H 11 0	
-9	264	273
-7	628	651
-3	492	511
-1	461	461
1	465	461
3	521	511
7	654	651
9	280	273

H	OBS	CALC
-8	142	116
-6	204	187
-4	174	142
0	625	588
4	181	142
6	224	187
8	151	116
	H 12 1	
-8	143	125
-6	141	126
-4	84	74
-2	163	135
2	257	245
	H 12 2	
-8	71	56
-7	74	63
-6	359	320
-4	231	192
-2	149	174
0	541	494
2	126	81
4	213	178
6	121	86